

Review

Not peer-reviewed version

---

# Applications of Hydrogels for Next-Generation Batteries

---

[Sabuj Chandra Sutradhar](#) , [Nipa Banik](#) , [Md. Shahriar Ahmed](#) , [Hohyoun Jang](#) , [Kyung-Wan Nam](#) , [Mobinul Islam](#) \*

Posted Date: 17 July 2025

doi: 10.20944/preprints202507.1432.v1

Keywords: hydrogels; synthesis methods; lithium-ion batteries; sodium ion batteries; zinc ion batteries; aluminum ion batteries; magnesium ion batteries



Preprints.org is a free multidisciplinary platform providing preprint service that is dedicated to making early versions of research outputs permanently available and citable. Preprints posted at Preprints.org appear in Web of Science, Crossref, Google Scholar, Scilit, Europe PMC.

Copyright: This open access article is published under a Creative Commons CC BY 4.0 license, which permit the free download, distribution, and reuse, provided that the author and preprint are cited in any reuse.

Disclaimer/Publisher's Note: The statements, opinions, and data contained in all publications are solely those of the individual author(s) and contributor(s) and not of MDPI and/or the editor(s). MDPI and/or the editor(s) disclaim responsibility for any injury to people or property resulting from any ideas, methods, instructions, or products referred to in the content.

Review

# Applications of Hydrogels for Next-Generation Batteries

Sabuj Chandra Sutradhar <sup>1</sup>, Nipa Banik <sup>2</sup>, Md. Shahriar Ahmed <sup>3</sup>, Hohyoun Jang <sup>1</sup>,  
Kyung-Wan Nam <sup>3</sup> and Mobinul Islam <sup>3,\*</sup>

<sup>1</sup> Department of Energy Materials Science and Engineering, Konkuk University, 268 Chungwon-aero, Chungju-si, Chungcheongbuk-do 27478, Republic of Korea

<sup>2</sup> Department of Applied Life Science, Konkuk University, 268 Chungwon-aero, Chungju-si, Chungcheongbuk-do 27478, Republic of Korea

<sup>3</sup> Department of Energy and Materials Engineering, Dongguk University-Seoul, Seoul 04620, Republic of Korea.

\* Correspondence: mobinsust@dongguk.edu; Tel.: +82-10-2159-4852.

## Abstract

Hydrogels have garnered significant attention as multifunctional materials in next generation rechargeable batteries due to their high ionic conductivity, mechanical flexibility, and structural tunability. This review presents a comprehensive overview of hydrogel types—including natural, synthetic, composite, carbon-based, conductive polymer, and MOF hydrogels—and their synthesis methods, such as chemical crosslinking, self-assembly, and irradiation-based techniques. Characterization tools like SEM, XRD, and FTIR are discussed to evaluate their microstructure and performance. In rechargeable batteries systems, hydrogels enhance ionic transport and mechanical stability, particularly in lithium-ion, sodium-ion, zinc-ion, magnesium-ion, and aluminum-ion batteries. Despite their advantages, hydrogels face challenges such as limited mechanical strength, reduced stability under extreme conditions, and scalability issues. Current research focuses on advanced formulations, self-healing mechanisms, and sustainable materials to overcome these limitations. This review highlights the pivotal role of hydrogels in shaping the future of flexible, high-performance, and environmentally friendly secondary batteries.

**Keywords:** hydrogels; synthesis methods; lithium-ion batteries; sodium ion batteries; zinc ion batteries; aluminum ion batteries; magnesium ion batteries

---

## 1. Introduction

The global energy landscape is undergoing a transformative shift driven by the urgent need to reduce carbon emissions, mitigate climate change, and transition toward sustainable energy systems. This transition demands the development of advanced materials and technologies capable of delivering high energy efficiency, long-term stability, and environmental compatibility. Energy storage and conversion devices—such as Metal-ion batteries [1–7], supercapacitors [8–10], fuel cells [11,12], and solar cells [13]—are at the forefront of this revolution, serving as critical enablers for renewable energy integration, electric mobility, and smart grid systems [14,15].

The advancement of energy technology hinges on the development of innovative materials that will significantly improve energy storage capacity for rechargeable batteries, enhance charge transport efficiency, and extend the lifespan of devices. [16]. In this context, hydrogels have emerged as a class of multifunctional materials with immense potential to address the limitations of conventional components in batteries. Hydrogels are three-dimensional, hydrophilic polymer networks capable of retaining large amounts of water while maintaining structural integrity. Their unique combination of mechanical flexibility, high ionic conductivity, tunable porosity, and

compatibility with diverse functional materials makes them ideal candidates for next-generation energy systems [17,18].

Recent research has demonstrated the versatility of hydrogels in various roles across energy devices. In batteries, hydrogels have been employed as solid-state electrolytes, separators, and electrode binders, offering improved ion transport, enhanced interfacial contact, and mechanical adaptability [19,20]. Hydrogel-based membranes have shown promise in facilitating proton conduction while maintaining hydration under operational conditions [21]. Moreover, hydrogels are being explored as electrolyte matrices in for energy storage material[22,23].The development of multifunctional hydrogels—engineered to exhibit properties such as self-healing[24], stretchability [25], thermo responsiveness [26], and shape memory[27]—has further expanded their applicability. These advanced hydrogels can adapt to mechanical deformation, recover from damage, and respond to environmental stimuli, thereby enhancing the durability and reliability of energy devices [28,29]. For instance, self-healing hydrogels can autonomously repair microcracks in electrodes or electrolytes, extending device lifespan [30,31]. Similarly, stretchable hydrogels enable the fabrication of flexible and wearable energy systems, aligning with the growing demand for portable and body-integrated electronics [32].

Despite these promising attributes, several challenges hinder the widespread adoption of hydrogel-based materials in commercial energy technologies[33]. Key issues include long-term stability under fluctuating environmental conditions, scalability of synthesis, and integration with existing device architectures [33–37]. Addressing these challenges requires interdisciplinary approaches that combine polymer chemistry, nanotechnology, electrochemistry, and device engineering. Strategies such as nanoparticle reinforcement, dual-network structuring, and hybridization with conductive polymers or carbon-based materials are being actively explored to enhance the mechanical and electrochemical performance of hydrogels [38–41]. Given the growing interest in hydrogel-based materials for battery applications, a systematic and up-to-date review is essential to consolidate recent findings and provide clarity on emerging trends. While many studies have examined the electrochemical and mechanical properties of hydrogels, the rapid development of multifunctional designs—such as self-healing, stretchable, and stimuli-responsive systems—necessitates a thorough reassessment of their roles in energy storage and conversion.

This review aims to provide a comprehensive overview of recent advances in hydrogel materials for battery materials. We discuss the fundamental properties that make hydrogels suitable for battery applications, their synthesis and functionalization strategies, and their roles in various energy systems. Furthermore, we highlight current limitations and outline future research directions, emphasizing the potential of multifunctional hydrogels to contribute meaningfully to the development of sustainable, high-performance energy technologies.

## 2. Hydrogels

### 2.1. Types of Hydrogels Used in Energy Applications

Hydrogels, with their three-dimensional polymeric networks and high water content, have become indispensable materials in energy storage and conversion technologies. Their ability to facilitate ion transport, maintain mechanical flexibility, and incorporate functional additives makes them ideal for use in batteries, supercapacitors, fuel cells, solar cells, and metal-air batteries. Based on their origin, composition, and functionalization, hydrogels used in energy applications can be broadly categorized into six main types: natural, synthetic, composite, carbon-based, conductive polymer, and metal-organic framework (MOF) hydrogels.

#### 2.1.1. Natural Hydrogels

Natural hydrogels are derived from biopolymers such as alginate, chitosan, and cellulose. These materials are biodegradable, biocompatible, and environmentally friendly, making them attractive for sustainable energy technologies. Their applications include use as electrolytes and separators in

batteries and supercapacitors, where their ionic conductivity and flexibility enhance device safety and performance [42]. However, their relatively low mechanical strength and limited electrochemical stability pose challenges for long-term use.

### 2.1.2. Synthetic Hydrogels

Synthetic hydrogels, such as those based on polyacrylamide (PAM), polyvinyl alcohol (PVA), and polyethylene glycol (PEG), offer greater control over chemical structure and physical properties. These hydrogels can be engineered to exhibit high ionic conductivity, mechanical robustness, and thermal stability. Their tunability makes them suitable for a wide range of energy devices, including lithium-ion and zinc-ion batteries, supercapacitors, and wearable electronics [42]. Despite their versatility, concerns about environmental impact and synthesis complexity remain.

### 2.1.3. Composite Hydrogels

Composite hydrogels are formed by incorporating functional fillers—such as carbon nanotubes (CNTs), graphene, MXenes, or metal oxides—into hydrogel matrices. These hybrids combine the ionic transport and flexibility of hydrogels with the electrical conductivity and mechanical strength of nanomaterials. Composite hydrogels have demonstrated enhanced electrochemical performance and are used in high-performance batteries, supercapacitors, and sensors [43]. Key challenges include achieving uniform dispersion of fillers and ensuring scalability.

### 2.1.4. Carbon-Based Hydrogels

Carbon-based hydrogels integrate carbon-rich materials like graphene, CNTs, activated carbon, or biomass-derived carbon into hydrogel networks. These materials offer high surface area, excellent electrical conductivity, and tunable porosity, making them ideal for energy storage applications. They are particularly effective in supercapacitors and flexible energy devices, where rapid charge transport and mechanical adaptability are essential [43]. However, issues such as filler aggregation and long-term stability must be addressed.

### 2.1.5. Conductive Polymer Hydrogels

Conductive polymer hydrogels (CPHs) incorporate intrinsically conductive polymers such as polyaniline (PANI), polypyrrole (PPy), and PEDOT into hydrogel matrices. These materials enable simultaneous ionic and electronic conduction, making them suitable for use as electrodes and electrolytes in supercapacitors, batteries, and flexible electronics. CPHs also exhibit self-healing, stretchability, and anti-freezing properties, which are advantageous for wearable and bio-integrated devices [43]. Their limitations include synthesis complexity and durability under repeated cycling.

### 2.1.6. MOF Hydrogels

Metal-organic framework (MOF) hydrogels combine the high surface area and tunable porosity of MOFs with the water-retentive and flexible nature of hydrogels. These hybrid materials are used in batteries, fuel cells, and catalytic systems, where they facilitate ion transport, enhance structural integrity, and support multifunctional performance [44]. MOF hydrogels are still in the early stages of development, with challenges related to MOF dispersion, scalability, and long-term stability.

Each type of hydrogel offers unique advantages and faces specific challenges (Table 1). The choice of hydrogel depends on the target application, desired properties, and operational environment. Continued innovation in hydrogel chemistry, nanomaterial integration, and device engineering will be essential to fully realize the potential of hydrogels in next-generation energy technologies.

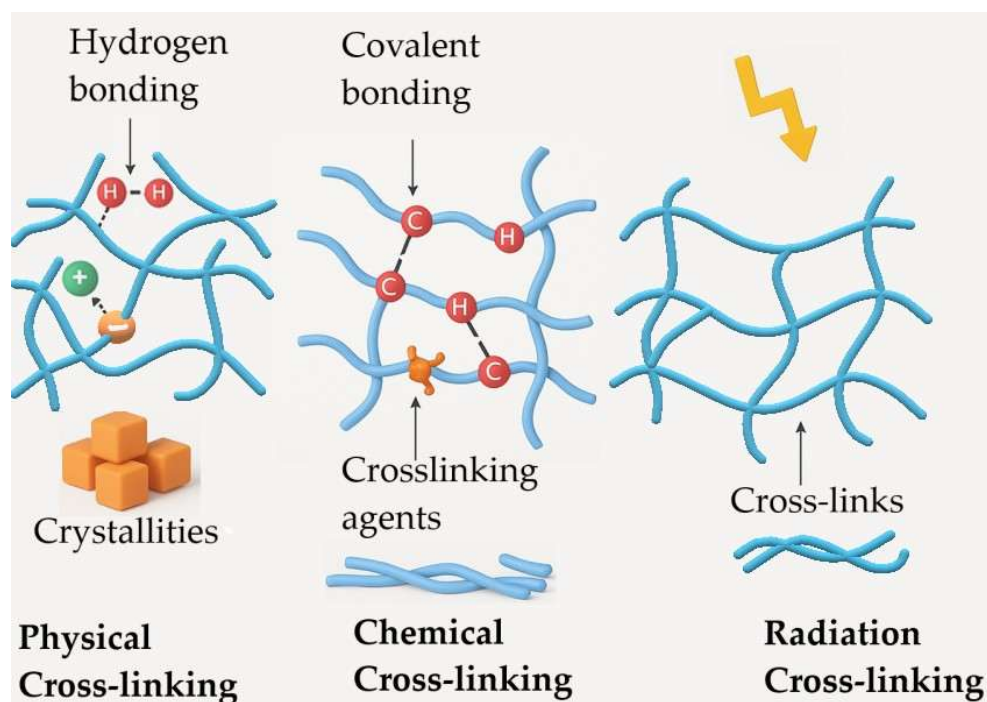
**Table 1.** Types of Hydrogels Used in Energy Applications.

Hydrogel Type	Source/Composition	Properties	Applications	Advantages	Challenges	Ref.
<b>Natural Hydrogels</b>	Alginate, chitosan, cellulose	Biocompatibility, biodegradability, high gelation ability	Electrolytes, separators in batteries and supercapacitors	Renewable, environmentally friendly	Mechanical strength, scalability	[42]
<b>Synthetic Hydrogels</b>	Polyacrylamide (PAM), polyethylene oxide (PEO), polyvinyl alcohol (PVA)	High water content, tunable mechanical properties, high ionic conductivity	Electrolytes, separators in batteries and supercapacitors	Customizable properties, high ionic conductivity	Environmental impact, mechanical robustness	[44]
<b>Composite Hydrogels</b>	Graphene oxide + polymer matrix, nanoparticles + polymer matrix	Enhanced mechanical properties, high electrical conductivity	Electrodes in batteries, supercapacitors	Enhanced properties, multifunctionality	Complexity in synthesis, cost	[44]
<b>Carbon-based Hydrogels</b>	Graphene, carbon nanotubes (CNTs)	High electrical conductivity, mechanical strength	Electrodes in batteries, supercapacitors	High electrical conductivity, mechanical strength	Scalability, cost	[45]
<b>Conductive Polymer Hydrogels</b>	Polyaniline, polypyrrole	High electrical conductivity, flexibility	Electrodes, sensors, supercapacitors	High electrical conductivity, flexibility	Stability, environmental impact	[46]
<b>Metal-Organic Framework (MOF) Hydrogels</b>	MOFs + polymer matrix	High porosity, tunable properties	Electrolytes, gas storage, sensors	High porosity, tunable properties	Synthesis complexity, cost	[47]

## 2.2. Preparation Methods of Hydrogels

Hydrogels are structured from polymer chains, and their characteristics are largely determined by the nature of the polymers employed. A defining feature of hydrogels is their remarkable capacity to absorb water; however, only specific polymers with suitable chemical functionalities can form effective hydrogel networks. Hydrogels are typically synthesized via two principal approaches: physical cross-linking and chemical cross-linking. Each method yields hydrogels with distinct structural and functional properties due to differences like the cross-links (Scheme 1).





**Scheme 1.** Overview of common Hydrogel Preparation Techniques.

Moreover, ionizing radiation—including X-rays, gamma rays, electron beams, ion beams, and high-energy ultraviolet light—can be employed to initiate polymerization and cross-linking processes. These radiations possess sufficient energy to cleave chemical bonds, thereby generating reactive species that drive polymerization or cross-linking. In polymerization, ionizing radiation facilitates the conversion of monomers into long polymer chains, a process known as radiation polymerization or radiation curing, which is widely applied in industries such as coatings, adhesives, and additive manufacturing.

### 2.2.1. Materials for Hydrogel Formation

Hydrogels can be synthesized from a wide range of materials, including synthetic polymers such as polyethylene oxide (PEO), polyvinyl alcohol (PVA), poly(acrylic acid) (PAA), and copolymers like poly(propylene fumarate-co-ethylene glycol) (P(PF-co-EG)). Additionally, polypeptides are increasingly used due to their biocompatibility and tunable properties. Natural polymers also play a significant role in hydrogel development, offering inherent bioactivity and biodegradability. These include agarose, alginate, chitosan, collagen, fibrin, gelatin, and hyaluronic acid.

### 2.2.2. Physical Cross-Linking

Physically cross-linked hydrogels are formed through non-covalent interactions among polymer chains, such as hydrogen bonding, van der Waals forces, hydrophobic interactions, and coordination bonds. Unlike chemically cross-linked hydrogels, these interactions are reversible, allowing the hydrogel to respond dynamically to environmental stimuli like temperature, pH, and ionic strength. This reversibility imparts unique properties such as self-healing and thermal sensitivity [48]. Hydrogels formed via physical cross-linking are typically short-lived in physiological conditions, with stability ranging from several days to about a month. Consequently, they are well-suited for applications requiring transient functionality, such as short-term drug delivery. Importantly, the absence of toxic cross-linking agents makes these hydrogels safer for clinical use.

Chitosan-based hydrogels, for example, can be physically cross-linked using small anionic molecules such as sulfates, phosphates, and citrates of platinum (Pt), palladium (Pd), and

molybdenum (Mo). The properties of the resulting hydrogels depend on factors such as the size and charge of the anions and the degree of deacetylation of chitosan. Overall, physical cross-linking methods offer advantages including high water sensitivity, thermal reversibility, and biocompatibility.

### 2.2.3. Chemical Cross-Linking

Chemical cross-linking involves the formation of covalent bonds between polymer chains, resulting in a stable and robust three-dimensional network. Unlike physical gels, chemically cross-linked hydrogels exhibit greater mechanical strength and long-term stability, and their performance is less influenced by environmental factors such as pH. This method allows for precise control over the hydrogel's structural and functional properties. Covalent cross-links are typically introduced through polymerization reactions or by using cross-linking agents. For instance, Tan et al. [49] developed injectable composite hydrogels by functionalizing hyaluronic acid with N-succinyl chitosan via a Schiff base reaction. Their study demonstrated that increasing the concentration of N-succinyl chitosan enhanced the compressive modulus, a key parameter for cartilage tissue engineering.

Similarly, Ito et al. [50] reported hydrogel formation using cellulose and alginate through analogous chemical mechanisms. Hydrogels can also be synthesized via Michael addition reactions, where amino groups react with vinyl groups of other polymers, resulting in enhanced mucoadhesive properties. Despite their advantages, chemically cross-linked hydrogels may require multistep synthesis and purification, and functionalization with reactive groups can sometimes introduce cytotoxicity.

### 2.2.4. Irradiation-Based Cross-Linking

Irradiation-based cross-linking has emerged as a promising strategy for hydrogel synthesis, particularly in applications where rapid gelation and cost-effectiveness are essential. This method utilizes light-sensitive functional groups in conjunction with ultraviolet (UV) or other forms of irradiation to induce cross-linking reactions, enabling the formation of hydrogels within a short time frame. Such an approach is especially advantageous in biomedical fields, including tissue engineering, drug delivery, and regenerative medicine [51,52]. Compared to conventional chemical cross-linking, irradiation-based methods offer several advantages in hydrogel synthesis. These include rapid gelation enabled by photo-reactive groups that initiate swift hydrogel formation upon UV exposure, significantly reducing processing time. Additionally, the elimination of costly chemical cross-linkers or catalysts contributes to greater cost efficiency, making irradiation-based techniques attractive for scalable and eco-friendly hydrogel production [53]. However, the effectiveness of this method depends on the compatibility of the photo-reactive moieties with the intended application, as well as the hydrogel's sensitivity to environmental factors such as light and temperature. A notable example is the work by Ono et al. [54], who developed UV-irradiated chitosan hydrogels using azide and lactose as photo-sensitive groups. These moieties were grafted onto the chitosan backbone, and upon UV exposure, the azide groups were converted into highly reactive nitrene intermediates. These intermediates subsequently reacted with amino groups on the chitosan chains, forming covalent bonds and establishing a stable three-dimensional network. Another approach, reported by Yoo et al. [55], involved the pre-functionalization of chitosan and Pluronic acid with photo-sensitive acrylate groups. Upon UV irradiation, these groups facilitated cross-linking and hydrogel formation. Despite its advantages, this method has certain limitations, including the need for light sensitizers, potential delays in irradiation, and localized heating effects, which may affect the uniformity and safety of the final hydrogel product.

## 2.3. Structural and Morphological Characterization

The structural and morphological properties of hydrogels are crucial in determining their performance in energy applications. Techniques such as scanning electron microscopy (SEM) and transmission electron microscopy (TEM) are widely used to analyze hydrogel porosity and microstructure [56]. Fourier-transform infrared spectroscopy (FTIR) and X-ray diffraction (XRD) help in identifying chemical compositions and crystalline structures, respectively [57]. Additionally, rheological measurements provide insights into the viscoelastic behavior of hydrogels, which is critical for their mechanical performance [58].

### 2.3.1. Microstructural Performance

The microstructure of hydrogels is a critical factor influencing their mechanical properties, degradation behavior, and molecular transport capabilities. Key parameters used to characterize hydrogel microstructure include the polymer volume fraction in the swollen state, mesh size, and the average molecular weight between cross-links. These structural features are influenced by the degree of cross-linking, the chemical nature of the monomers, and environmental conditions such as pH, temperature, and ionic strength [59]. Mesh size, in particular, governs the hydrogel's mechanical strength, permeability, and ability to release encapsulated molecules. By tuning these parameters, hydrogels can be tailored for specific biomedical applications, including drug delivery, tissue scaffolding, and wound healing.

Zhang et al. [60] used scanning electron microscopy (SEM) to examine hydrogels cross-linked with microbial transglutaminase (MTG). The M7-crosslinked variant exhibited a smoother, denser surface and a distinctive honeycomb-like internal structure, attributed to combined hydrogen bonding, hydrophobic interactions, and covalent cross-linking (Figure 1a ).

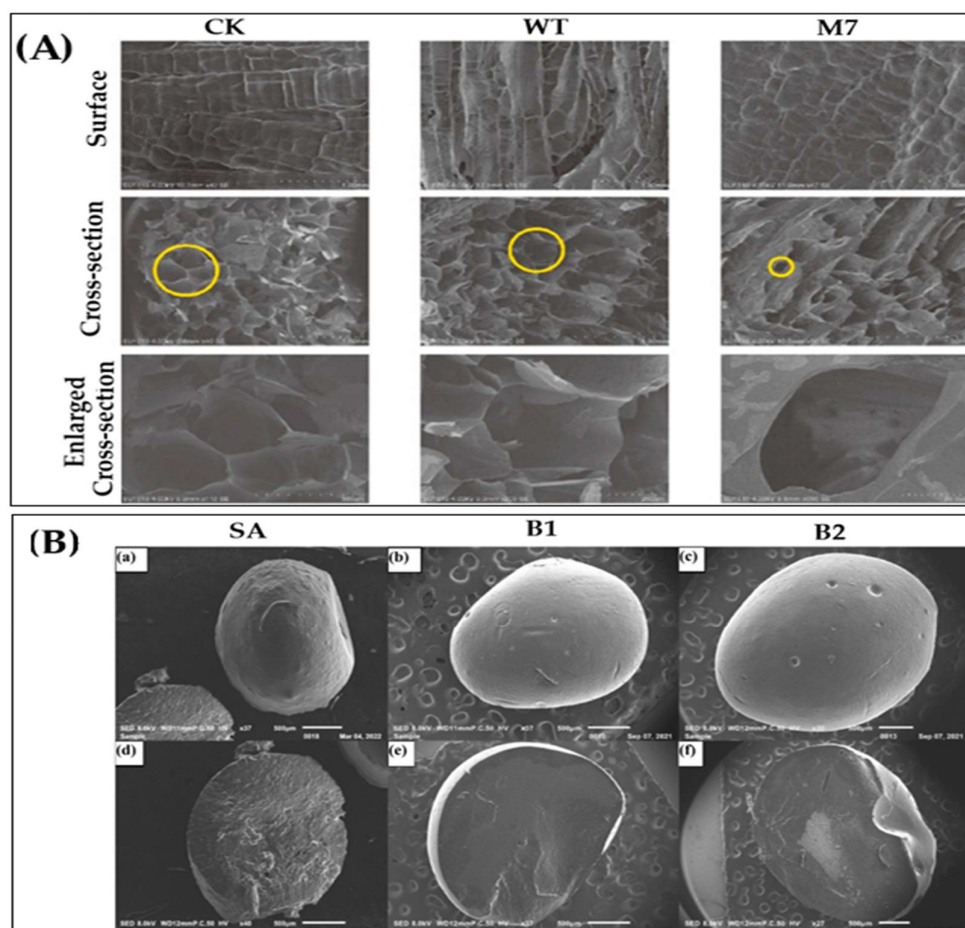




**Figure 1.** (A) SEM micrographs showing surface morphology of hydrogels before and after enzymatic modifications, reproduced with permission from ref. [60], (B) surface and cross-sectional views of hydrogel beads: (a,d) SA; (b,e) B1; (c,f) B2, reproduced with permission from ref. [61], Elsevier.

Camerco et al. [61] compared sodium alginate (SA) hydrogel beads with those modified by thermosensitive materials (TSM). SEM images showed that SA beads had rougher surfaces and more porous interiors, while SA-TSM beads exhibited smoother surfaces and more uniform internal structures. The bead size increased with TSM due to higher viscosity, and the sphericity factor (SF) was lower in SA-TSM beads, indicating improved cross-linking and shape uniformity (Figure 1b-g).

### 2.3.2. Morphology Study

Morphological characterization is essential for understanding the structural and functional properties of hydrogels. Techniques such as Field Emission Scanning Electron Microscopy (FE-SEM), Environmental Scanning Electron Microscopy (ESEM), and Transmission Electron Microscopy (TEM) are commonly employed to analyze hydrogel surfaces and internal architectures.

FE-SEM provides high-resolution images of dehydrated hydrogel surfaces, revealing features like porosity, roughness, and structural defects [62]. Polyaniline-polyvinyl alcohol (PANI-PVA) hydrogel, synthesized via in situ polymerization of aniline in acidic PVA solution followed by freeze-thaw gelation, was reported as a self-supported electrode for supercapacitors [63]. FESEM analysis revealed that pure PVA hydrogel exhibits a nanoporous structure, while PANI-PVA retains this morphology with uniformly distributed PANI nanoaggregates (nanorods, nanosheets, nanoparticles). These aggregates enhance ion/electron transport, improving electrochemical performance [63,64].

TEM offers nanoscale insights into the internal structure, including particle size, shape, and distribution of embedded nanoparticles [65]. For instance, Huang et al. [64] developed a MnO<sub>2</sub>-embedded 3D porous polyaniline (PANI) hydrogel electrode for supercapacitor applications. FE-SEM revealed a robust coral-like surface structure, while TEM showed uniformly distributed MnO<sub>2</sub> nanoparticles coated with a protective PANI layer (20–50 nm). This architecture facilitated efficient electron transfer, resulting in a specific capacitance of 293 F/g at 1.5 mg/cm<sup>2</sup> loading, which decreased to 258 F/g at 10.8 mg/cm<sup>2</sup> due to increased mass loading.

### 2.3.3. Mechanical Properties and Performance of Hydrogels

The mechanical behavior of hydrogels is a critical factor in determining their suitability for biomedical and engineering applications. These properties are typically evaluated using standard techniques such as tensile, compression, indentation, bulge, and cyclic testing. Tensile tests provide insights into elasticity and strength, while compression tests assess deformation under load. Indentation and bulge tests help characterize localized stiffness and membrane behavior, respectively. Cyclic or fatigue testing evaluates durability under repeated stress, which is essential for long-term applications.

Hou et al. [66] demonstrated that PVA-CMC hydrogels possess excellent mechanical performance for soft strain sensors. Cyclic stress-strain tests showed consistent behavior across multiple loading cycles, confirming their durability and elasticity (Figure 2 a-o). PVA-based hydrogels demonstrate remarkable mechanical resilience, especially when modified with additives like DMSO and carboxymethyl cellulose (CMC). A hydrogel strip (3.5 mm thick, 4.5 mm wide) was able to support 1 kg without damage and maintained its integrity under stretching, twisting, knotting, and drilling (Figure 2a-d).

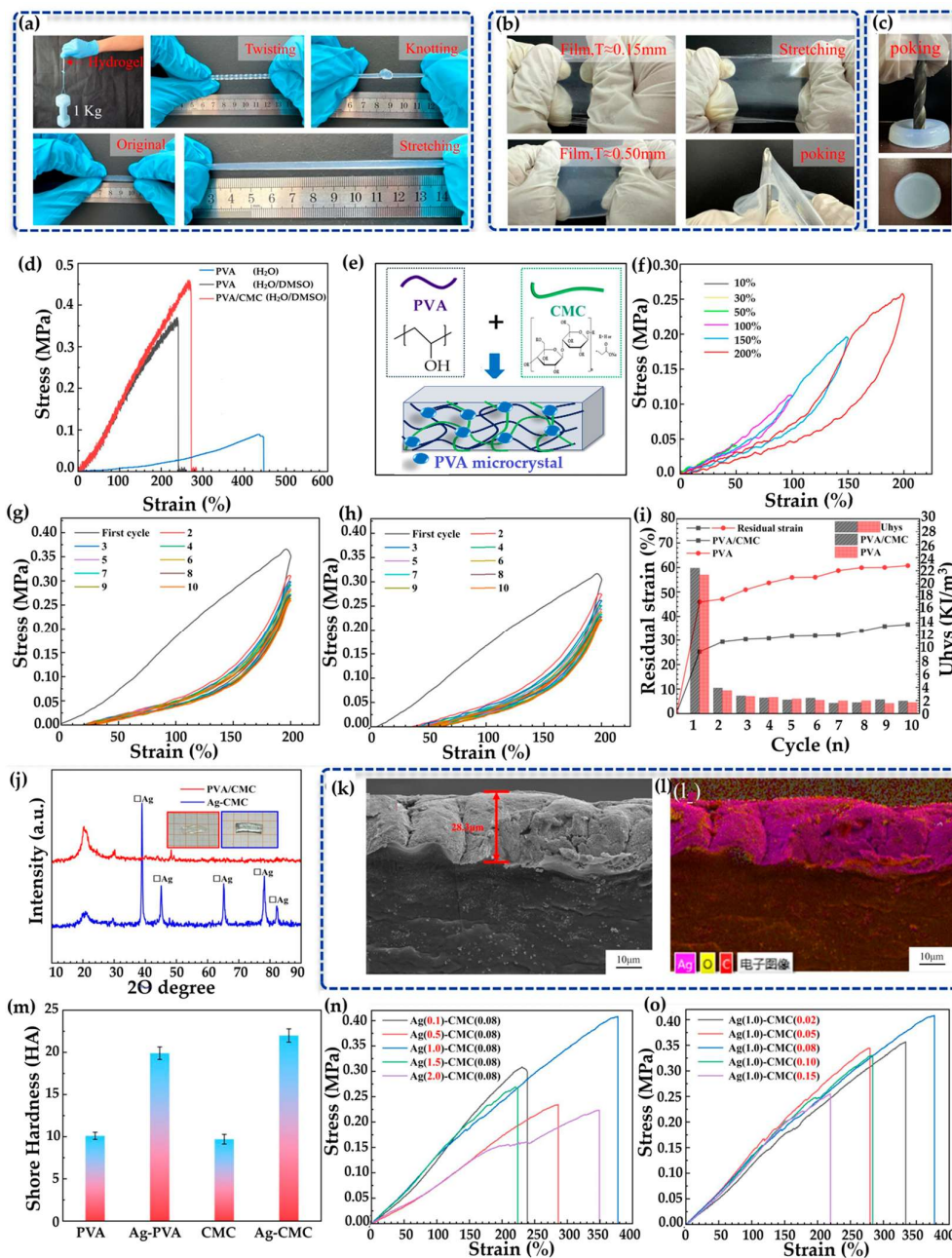


**Figure 2.** (a) Mechanical flexibility of PVA/CMC hydrogel demonstrated through hanging, twisting, knotting, and stretching. (b, c) Stretching and puncture resistance of PVA/CMC hydrogel film and block, respectively. (d) Tensile stress–strain profiles of PVA-CMC (H<sub>2</sub>O/DMSO), pure PVA (H<sub>2</sub>O/DMSO), and pure PVA (H<sub>2</sub>O) hydrogels. (e) Schematic of freeze-molded CMC and PVA chain arrangement. (f) Loading–unloading behavior of PVA-CMC hydrogels under varying strain levels. (g–i) Cyclic loading–unloading, residual strain, and energy dissipation of PVA-CMC and pure PVA hydrogels. (j) XRD patterns of PVA/CMC and Ag-CMC conductive hydrogels. (k, l) Cross-sectional morphology of Ag-CMC conductive hydrogels. (m) Shore hardness of PVA and PVA-CMC hydrogels before and after silver reduction. (n, o) Tensile stress–strain curves of conductive hydrogels with varying AgNO<sub>3</sub> and VC concentrations, reproduced with permission from ref. [66], Elsevier.

The addition of DMSO reduced the fracture strain of pure PVA from 446.48% to 241.18%, while increasing its fracture stress to 0.366 MPa. Incorporating CMC further enhanced both strength and strain, reaching 0.453 MPa and 272.13%, respectively (Figure 3e). Cyclic testing revealed stable hysteresis behavior, indicating excellent fatigue resistance and energy dissipation, particularly due

to increased crosslinking density from DMSO (Figure 2f–i). Hardness tests showed that Ag-CMC hydrogels had superior values compared to pure PVA, and the Ag(1.0)-CMC(0.08) formulation achieved optimal mechanical strength and low electrical resistance (Figure fm–o).

### 2.3.4. Fourier Transform Infrared Spectroscopy (FTIR)

FTIR spectroscopy is a powerful analytical technique used to identify the chemical structure and bonding characteristics of hydrogel materials. It works by detecting the absorption of infrared light at specific frequencies corresponding to the vibrational modes of chemical bonds. Each functional group within a molecule absorbs IR radiation at characteristic frequencies, allowing researchers to determine the presence and interactions of these groups within hydrogel systems [67].

Medha et al. [68] analyzed FTIR spectra of chitosan, starch, chitosan-starch hydrogel, and cefixime-loaded hydrogel. Broad absorption bands between 3300 and 2850  $\text{cm}^{-1}$  were observed, corresponding to  $-\text{OH}$ ,  $-\text{NH}_2$ , and  $-\text{CH}$  stretching vibrations. Chitosan exhibited peaks at 1645  $\text{cm}^{-1}$  ( $\text{C}=\text{O}$  stretching), 1548  $\text{cm}^{-1}$  ( $-\text{NH}$  bending), and 1380  $\text{cm}^{-1}$  ( $-\text{CH}_3$  deformation), while starch showed weaker signals at 1650  $\text{cm}^{-1}$  and deformation bands at 1436 and 1340  $\text{cm}^{-1}$ . The chitosan-starch hydrogel displayed a band at 1653  $\text{cm}^{-1}$ , indicating successful grafting and crosslinking. Cefixime-loaded hydrogels showed distinct peaks at 1768, 1669, 1588, 1537, and 1384  $\text{cm}^{-1}$ , suggesting drug-polymer interactions (Figure 3i (a–e)).

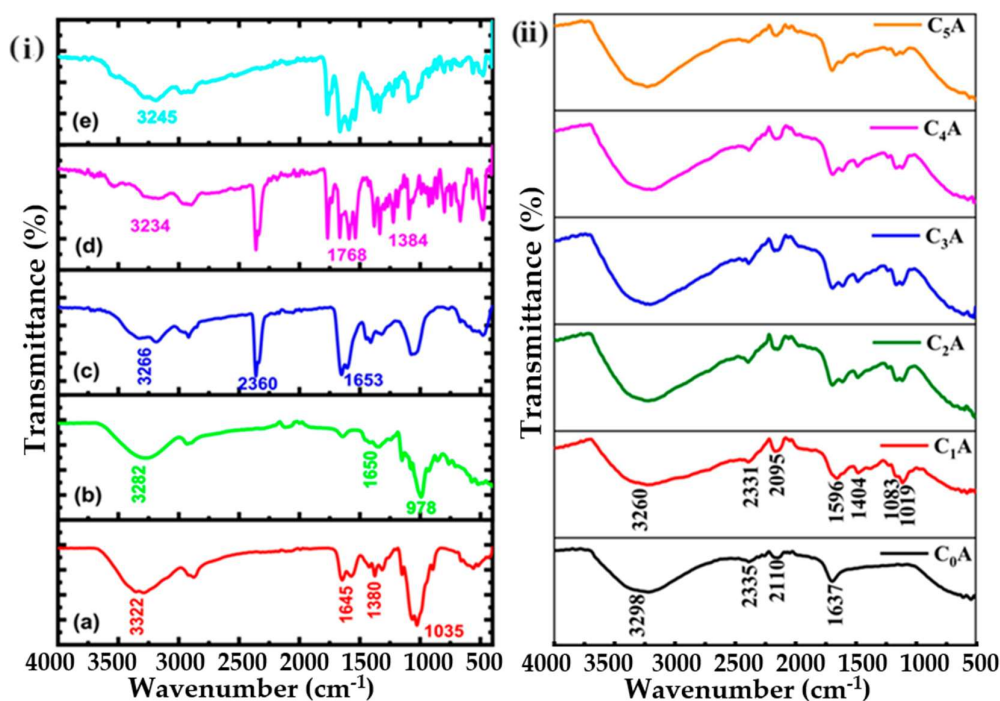


**Figure 3.** (i) FTIR spectra illustrating the characteristic peaks of (a) pure chitosan, (b) native starch, (c) chitosan-starch composite hydrogel, (d) cefixime, and (e) cefixime-incorporated hydrogel, reproduced with permission from ref. [68], Elsevier. (ii) FTIR profiles of chitosan/alginate hydrogel systems, reproduced with permission from ref. [69], Elsevier.

Enoch et al. [69] further investigated chitosan/alginate hydrogels at varying concentrations. The alginate hydrogel (C<sub>0</sub>A) showed peaks at 3298  $\text{cm}^{-1}$  ( $\text{O}-\text{H}$  stretching), 2110  $\text{cm}^{-1}$  ( $\text{C}-\text{H}$  stretching), 2335  $\text{cm}^{-1}$  ( $\text{CO}_2$ ), and 1637  $\text{cm}^{-1}$  ( $\text{COO}^-$  stretching). Chitosan/alginate composites (C<sub>1</sub>A to C<sub>5</sub>A) exhibited overlapping  $\text{O}-\text{H}$  and  $\text{N}-\text{H}$  stretching bands around 3260  $\text{cm}^{-1}$ , with additional peaks at 1019 and 1083  $\text{cm}^{-1}$  ( $\text{C}-\text{O}$  and  $\text{C}-\text{H}$  stretching), and 1404 and 1596  $\text{cm}^{-1}$  indicating amine-aldehyde interactions and  $\text{COO}^-$  stretching (Figure 3ii).

### 2.3.5. Viscoelastic Properties

Viscoelasticity is a defining mechanical characteristic of hydrogels, reflecting their ability to exhibit both elastic and viscous responses under deformation. These properties are typically assessed through rheological methods such as compression testing and oscillatory shear analysis. The viscoelastic behavior of hydrogels can be finely tuned by adjusting polymer and crosslinker concentrations, which directly influence stiffness, elasticity, and energy dissipation [70].

Zhang et al. [71] demonstrated that S-Alg hydrogels exhibited low tensile modulus ( $2.7 \pm 0.7$  kPa) but high elongation (224%), whereas D-Alg hydrogels showed significantly higher tensile ( $134.6 \pm 6.2$  kPa) and compression modulus ( $453.9 \pm 16.9$  kPa), indicating enhanced stiffness. Viscoelastic analysis revealed that both hydrogels maintained a wide linear viscoelastic range up to 10% strain, with D-Alg displaying a higher storage modulus ( $G'$ ) than loss modulus ( $G''$ ), consistent with robust network structures (Figure 4a-d)

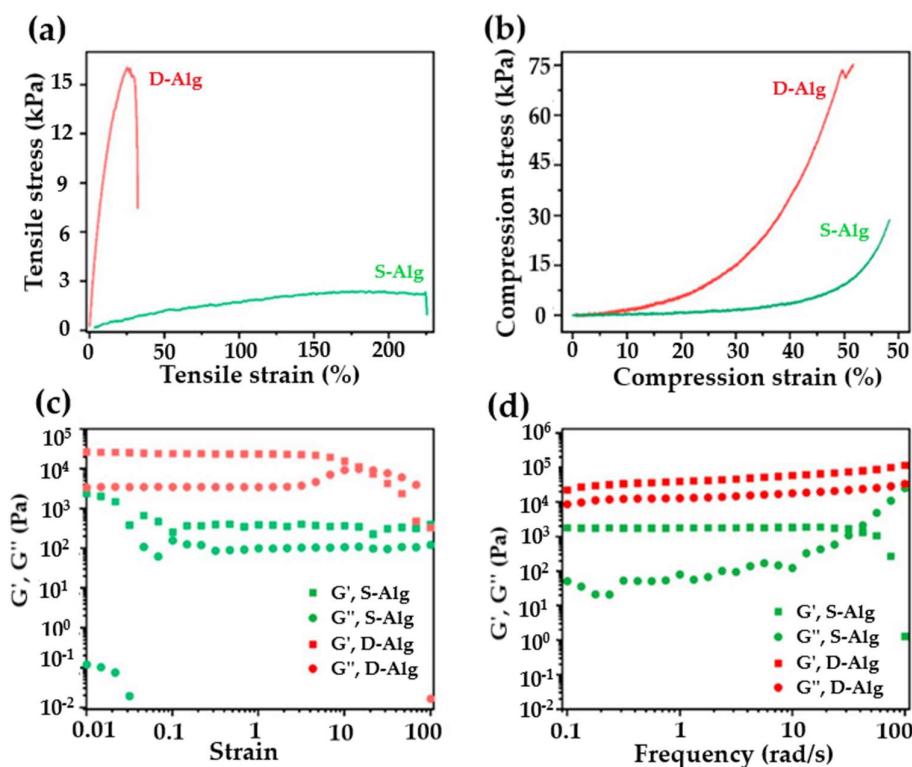


**Figure 4.** Mechanical and rheological characterization of S-Alg and D-Alg hydrogels (a) tensile, (b) compression, (c) amplitude, and (d) frequency sweep tests, reproduced with permission from ref. [71], Elsevier.

For example, increasing the concentration of glutaraldehyde in gelatin hydrogels enhances stiffness and shifts the material toward a more elastic regime. Similarly, modifying the viscosity of the aqueous phase with dextran in agarose or polyacrylamide hydrogels allows for control over viscoelasticity while maintaining a stable elastic modulus—an important consideration for biomedical applications.

In physically or non-covalently crosslinked hydrogels, viscoelasticity arises from dynamic molecular mechanisms. Crosslinkers may temporarily detach under stress, allowing the polymer matrix to flow and then reattach, as observed in collagen, alginate, and PEG-based gels. Additional contributions from polymer entanglement and protein unfolding further enhance energy dissipation and reversible deformation [72]. Even in well-crosslinked systems, the high water content contributes to a measurable loss modulus, enabling viscoelastic behavior without permanent deformation.

## 3. Hydrogel-Based Materials in Energy Storage Applications



### 3.1. Hydrogels in Batteries

Rechargeable batteries are central to modern energy storage, typically composed of a cathode, anode, and electrolyte. These components work together to store and transfer charge carriers—commonly alkaline metal ions like  $\text{Li}^+$ ,  $\text{Na}^+$ ,  $\text{Zn}^{2+}$ ,  $\text{Mg}^{2+}$  and  $\text{Al}^{3+}$ —during charge and discharge cycles (Figure 5). These ions are favored for their high reactivity, low reduction potential, and high specific capacity, enabling efficient energy conversion and storage.

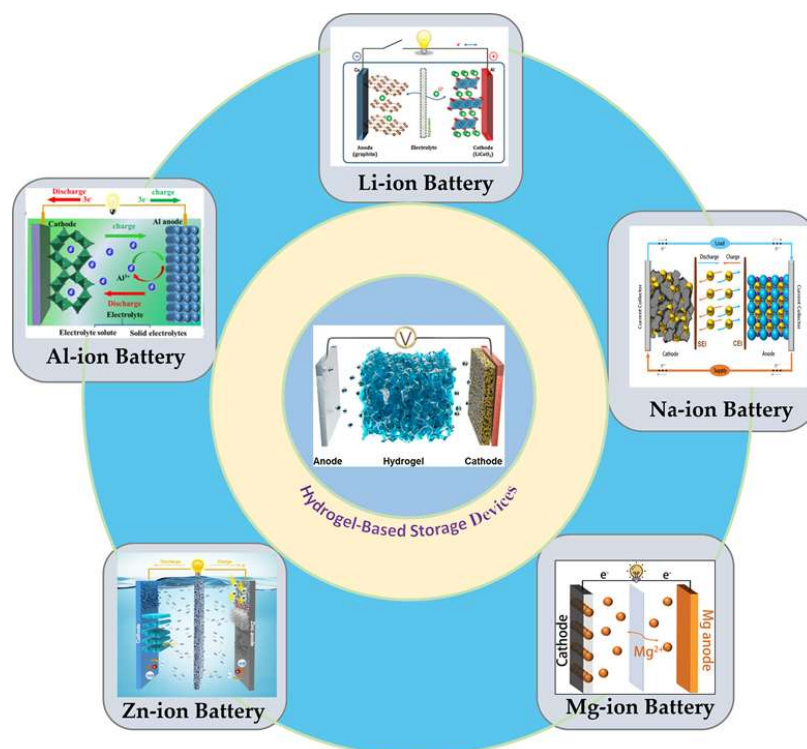


**Figure 5.** Conceptual illustration of hydrogel-based materials integrated into advanced energy storage technologies, adapted and redrawn from sources [73–78].

However, conventional lithium-ion batteries are nearing their performance limits, with energy densities below  $500 \text{ Wh kg}^{-1}$ , rising material costs, and persistent safety concerns [79]. To address these issues, researchers have explored multivalent ions such as  $\text{Mg}^{2+}$ ,  $\text{Ca}^{2+}$ ,  $\text{Zn}^{2+}$ , and  $\text{Al}^{3+}$ , which offer higher charge densities and lower cost. Yet, practical implementation remains limited due to challenges in ion mobility and electrode compatibility [80].

Hydrogels have emerged as a promising solution to these limitations. Their unique multifunctionality—including easy fabrication [81], tunable ionic and electronic conductivity [81,82], ability to form stable solid-electrolyte interphases [83,84], and enhanced mechanical strength [85,86]—makes them ideal candidates for improving battery performance. Hydrogels can be engineered into electrodes, binders, and electrolytes, offering improved charge transport, mechanical integrity, and interface stability.

In the following sections, we explore how hydrogel-based materials are being applied across battery components, highlighting their role in hydrogel-based electrodes, binders, electrolytes, and other hydrogel-derived multifunctional materials.

### 3.2. Hydrogels in Li-ion Batteries

#### 3.2.1. Hydrogel-Derived Electrodes



Electrodes are the heart of rechargeable batteries, where redox reactions occur to store and release energy. For optimal performance, electrodes must support fast ion and electron transport while maintaining mechanical integrity and strong connectivity between active materials and current collectors. However, conventional electrodes fabricated via solid-state reactions and thermal annealing often suffer from particle agglomeration and irregular morphologies, which hinder conductivity and ion diffusion [87]. To address this, Tang et al. [88] developed a continuous  $\text{Li}_4\text{Ti}_5\text{O}_{12}$  (LTO) framework by crosslinking LTO with reduced graphene oxide (rGO) colloids. The solution-processable ink was coated onto a current collector, forming a highly conductive network (Figure 6i, ii). The rGO nanosheets bridged LTO particles and the current collector, while the mesoporous structure shortened Li-ion diffusion paths, enhancing overall performance.

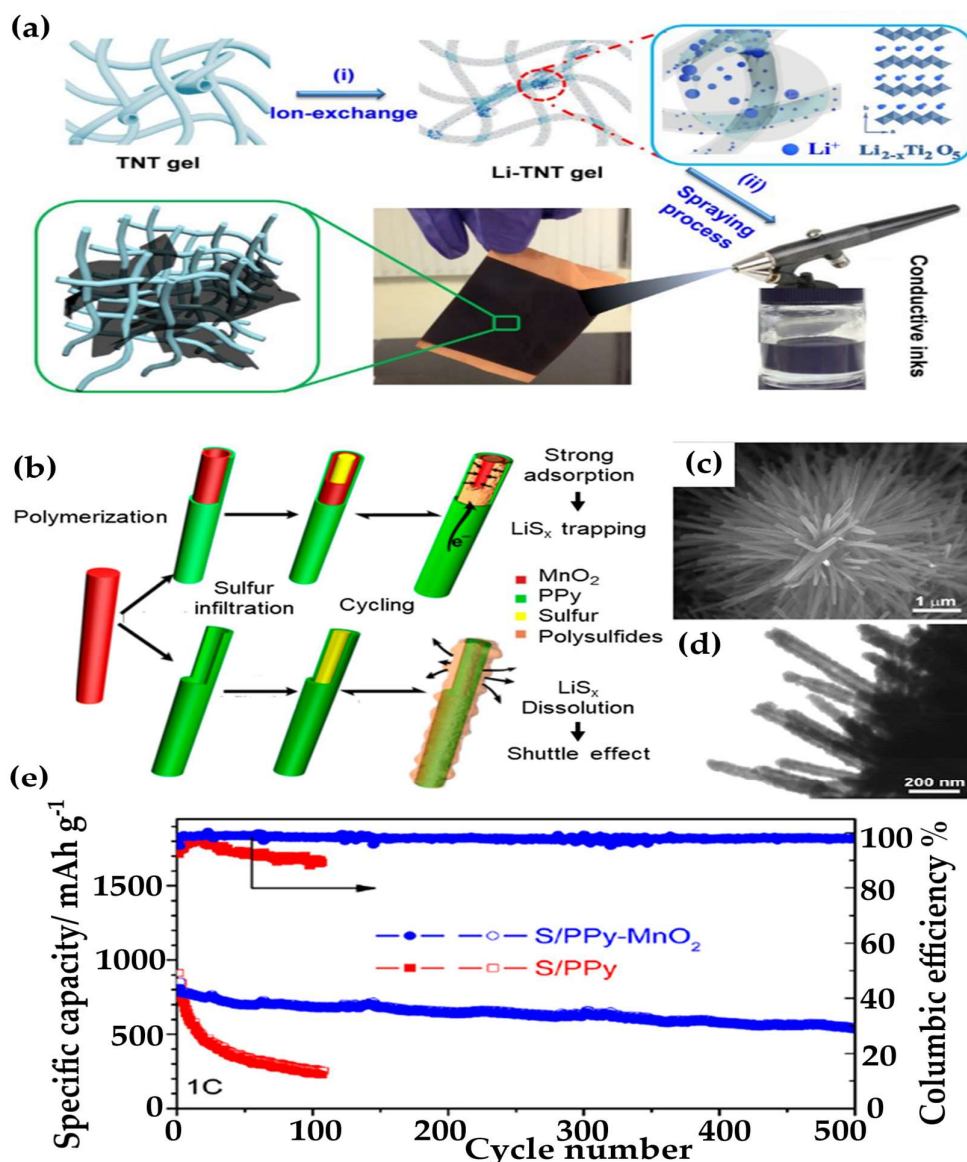


**Figure 6.** (a) Stepwise formation of conductive Li-TNT ink (i) ion exchange, (ii) spray coating on Cu foil, followed by thermal conversion to LTO/rGO, adapted with permission from ref. [88], Wiley & Sons. (b) Schematic of S/PPy-MnO<sub>2</sub> composite synthesis and its electrochemical benefits during cycling. (c, d) SEM and TEM images showing MnO<sub>2</sub> nanowires and PPy-MnO<sub>2</sub> nanotubes, respectively. (e) Comparison of sulfur electrodes encapsulated with PPy-MnO<sub>2</sub> nanotubes versus pure PPy nanotubes, adapted with permission from ref. [89], copyright© 2016 American Chemical Society.

Hydrogel-template methods have also been applied to synthesize nanosized electrode materials with high surface areas, such as  $\text{MnO}_2$ ,  $\text{TiO}_2$ ,  $\text{LiFePO}_4$ , and  $\text{Fe}_2\text{O}_3$  [90–93]. These structures increase reaction sites and facilitate charge transfer, which is especially beneficial for low-conductivity materials like  $\text{LiFePO}_4$ . Hasegawa et al. [94] demonstrated this by fabricating meso-/macroporous  $\text{LiFePO}_4$  using hydrogels derived from metal precursors and polymers (PEO and polyvinylpyrrolidone). The carbon coating from polyvinylpyrrolidone improved electronic conductivity, resulting in enhanced electrochemical performance.

Beyond geometric advantages, hydrogel-based composites offer solutions for more complex systems like lithium–sulfur (Li–S) batteries, which promise high specific capacities (sulfur:  $1675 \text{ mAh g}^{-1}$ ; Li metal:  $3860 \text{ mAh g}^{-1}$ ). However, sulfur's poor conductivity, polysulfide dissolution, and volume-change degradation remain major challenges [95,96]. To mitigate these issues, Zhang et al. [89] designed a composite hydrogel-derived electrode using  $\text{MnO}_2$  nanowires as oxidants for polypyrrole (PPy) polymerization (Figure 6a–c). After sulfur infiltration, the resulting S/PPy– $\text{MnO}_2$  electrode exhibited excellent Coulombic efficiency, cycling stability, and rate capability (Figure 6d). The  $\text{MnO}_2$  nanowires effectively trapped polysulfides, while the conductive PPy hydrogel facilitated rapid electron transport.

Silicon is a highly promising anode material for lithium-ion batteries due to its high theoretical capacity. However, its practical application is hindered by severe volume expansion and poor cycling stability. To address these challenges, a novel strategy was proposed using a fibrin biopolymer hydrogel as a template to fabricate a three-dimensional (3D) interconnected Si@C framework (Figure 7a) [97].

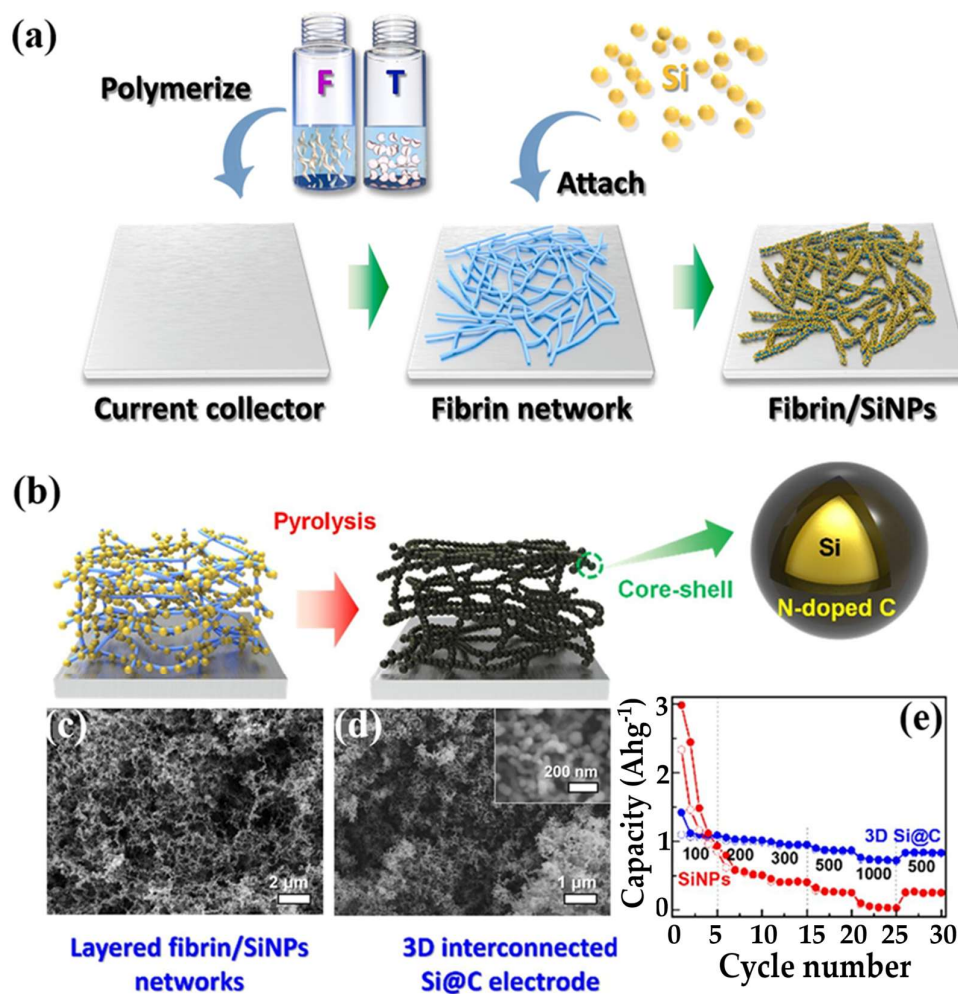


**Figure 7.** (a) Schematic of the fibrin/SiNPs assembly, (b) 3D Si@C electrodes, (c,d) SEM/TEM images before and after pyrolysis, respectively, (e) rate performance comparison between 3D Si@C and conventional SiNPs electrodes, reproduced with permission from ref. [97], Elsevier.

This binder- and additive-free architecture utilizes strong hydrogen bonding between fibrin amide groups and hydroxyl-functionalized silicon nanoparticles (SiNPs), enabling uniform dispersion of SiNPs within a nitrogen-doped amorphous carbon matrix. Pyrolysis of the hydrogel preserves the porous 3D structure and introduces pyridinic and pyrrolic nitrogen species, which enhance both electronic conductivity and lithium storage capability (Figure 7 b-d). The resulting 3D Si@C electrode delivers a high specific capacity of  $730 \text{ mAh g}^{-1}$  at  $1000 \text{ mA g}^{-1}$  and retains 54% of its capacity after 500 cycles at  $500 \text{ mA g}^{-1}$  significantly outperforming conventional SiNP-based composites (Figure 7e). This scalable and sustainable design offers a promising route for advanced electrode architectures, with further optimization possible through control of fibrin mesh size, Si loading, and carbon crystallinity.

### 3.2.2. Hydrogel-Derived Binders

The rising demand for high-energy-density batteries in electric vehicles, wearable electronics, and grid storage has intensified the need for electrodes with high capacity, flexibility, and long-term cycling stability [98–100]. However, silicon (Si) and sulfur-based electrodes suffer from severe volume expansion during lithiation/delithiation, leading to mechanical degradation, poor conductivity, and rapid capacity fading [101]. To address these challenges, various research groups have developed hydrogel-based binders and carbon frameworks that offer mechanical flexibility, strong adhesion, and the ability to accommodate volume changes. One notable example is the hydrogel binder developed. A chitosan (CS)-based binder crosslinked with glutaraldehyde (GA), shown in Figure 8a, forms a robust 3D network that enhances mechanical stability. This system delivered  $2,782 \text{ mAh g}^{-1}$  initially and maintained  $1,969 \text{ mAh g}^{-1}$  after 100 cycles [102].

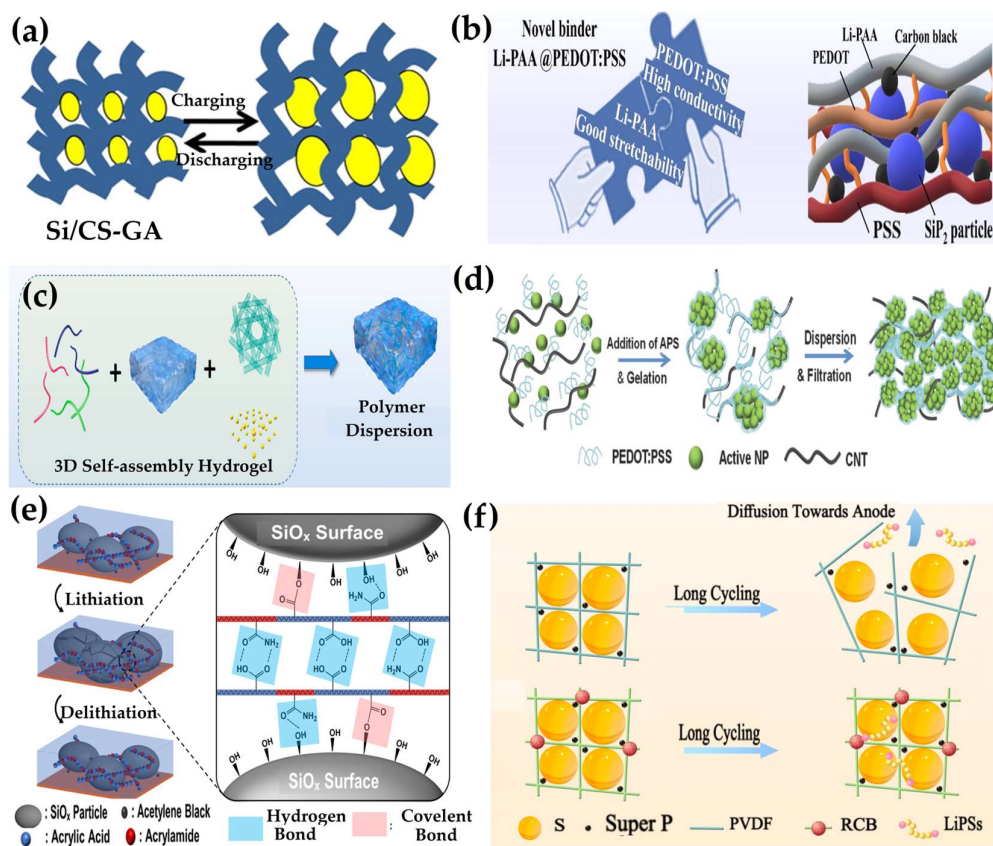




**Figure 8.** Schematic representations of various hydrogel-based binder systems designed for silicon anodes, highlighting in-situ polymerization approaches and structural strategies to mitigate volume expansion during cycling. (a) Charge/discharge mechanism of Si/CS-GA anodes, adapted with permission from ref. [102], copyright © 2016, American Chemical Society ; (b–f) diverse hydrogel architectures including CHSP and RCB binders, demonstrating enhanced mechanical integrity and electrochemical performance. Adapted with permission from ref. [103,104], Elsevier; ref. [105,106], American Chemical Society; and ref. [107], Wiley & Sons.

In another approach, Wu et al. [108] developed a hierarchical hydrogel framework (Figure 8b) by incorporating a conducting polymer. This 3D network provided continuous electrical pathways and space for Si expansion, achieving over 90% capacity retention after 5,000 cycles at  $6.0 \text{ A g}^{-1}$ .

To further enhance flexibility and conductivity, Liu et al. [103] designed a stretchable binder, Li-PAA@PEDOT:PSS which accommodated volume changes in  $\text{SiP}_2$  anodes and supported self-healing. A double-network hydrogel composed of polyvinyl alcohol (PVA) and sodium alginate (SA), reinforced with hydroxypropyl cellulose (HPC), formed a porous structure (Figure 8c) that buffered Si expansion and improved ion transport [104].

Beyond these, Chen et al. [107] introduced a hybrid hydrogel system combining carbon nanotubes (CNTs) and a conductive polymer (Figure 8d). This design improved mechanical strength and ion transport, demonstrating excellent performance in both  $\text{TiO}_2$  and SiNP electrodes. A copolymer binder made from acrylamide and acrylic acid (Figure 8e) formed a covalent–noncovalent elastic network, significantly enhancing the capacity of  $\text{SiO}_x$  anodes to  $734 \text{ mAh g}^{-1}$  after 300 cycles. Polyimine binders also showed promise, achieving  $804.4 \text{ mAh g}^{-1}$  with 82.4% retention after 1,000 cycles, and  $2,114 \text{ mAh g}^{-1}$  over 200 cycles in high-loading Si electrodes [105].

Inspired by spider webs, a tapioca–PAA (TA–PAA) binder was developed with high viscoelasticity and self-healing properties. This binder enabled a SiO anode to deliver  $901.2 \text{ mAh g}^{-1}$  over 1,200 cycles and  $619.2 \text{ mAh g}^{-1}$  at a high rate of  $5 \text{ A g}^{-1}$  [109]. Additionally, an alginate hydrogel crosslinked with  $\text{Ca}^{2+}$  ions improved the performance of Si/C anodes [110]. For wearable electronics, Wang et al. [111] created an ultrasoft, all-hydrogel coaxial fiber battery with a low Young's modulus, achieving  $84.8 \text{ mAh g}^{-1}$  at  $0.5 \text{ A g}^{-1}$  and maintaining stable performance under deformation.

In parallel, lithium–sulfur (Li–S) batteries face their own set of challenges, including sulfur's poor conductivity and up to 80% volume expansion during cycling [112]. To address this, Zhang et al. [106] developed a responsive/confinement network blend (RCB) binder (Figure 8f) using hyaluronic acid and a tetrazole-functionalized copolymer. This dual-network structure mimics muscle tissue, coordinating mechanical stress and accommodating sulfur expansion. Even with just 5 wt% binder, the system showed excellent cycling and rate performance under high sulfur loading.

Hydrogels have also been explored as carbon sources. Upon pyrolysis, they form 3D porous carbon frameworks ideal for embedding nanomaterials [94]. Liu et al. [113] fabricated a carbon–MOF composite electrode with ZIF-67 and HKUST-1, achieving an areal capacity of over  $16 \text{ mAh cm}^{-2}$  and 82% retention after 300 cycles. Xu et al. [114] embedded Sn nanoparticles in hydrogel-derived carbon (Sn@PHDC), which improved lithium-ion diffusion, reduced charge transfer resistance, and enhanced cycling stability.

Together, these innovations highlight the versatility and effectiveness of hydrogel-based binders and frameworks in addressing the mechanical and electrochemical limitations of both Si and sulfur electrodes. They offer scalable, multifunctional solutions for the development of next-generation, high-performance energy storage systems.

### 3.2.3. Hydrogel Electrolytes for Aqueous Lithium-Ion Batteries

Hydrogels have gained significant attention in lithium-ion battery (LIB) research due to their tunable porous structures, which facilitate lithium-ion diffusion and reduce transport resistance [115,116]. These properties enhance electrochemical performance by enabling rapid ion transport and stable electrode–electrolyte interfaces. Hydrogels can also be engineered to exclude free water, making them compatible with electrodes and current collectors, and are increasingly used as solid

electrolytes and separators [117,118]. In aqueous LIBs, which use water-based electrolytes for improved safety and environmental compatibility, hydrogels help mitigate the narrow electrochemical stability window ( $\sim 1.23$  V) that limits energy density [119].

To address these limitations, researchers have developed functional hydrogels tailored for specific challenges such as flame retardancy, thermal protection, mechanical flexibility, and electrochemical stability. Yang et al. [120] created a flame-retardant separator using a boron nitride (BN) aerogel synthesized from a melamine–boric acid (MBA) supramolecular hydrogel. Combined with bacterial cellulose (BC), the BN/BC composite (Figure 9 a) exhibited excellent flame resistance, electrolyte wettability, and mechanical strength. When used in LIBs, it delivered a high specific discharge capacity of  $146.5 \text{ mAh g}^{-1}$  and showed only 0.012% capacity degradation per cycle over 500 cycles .

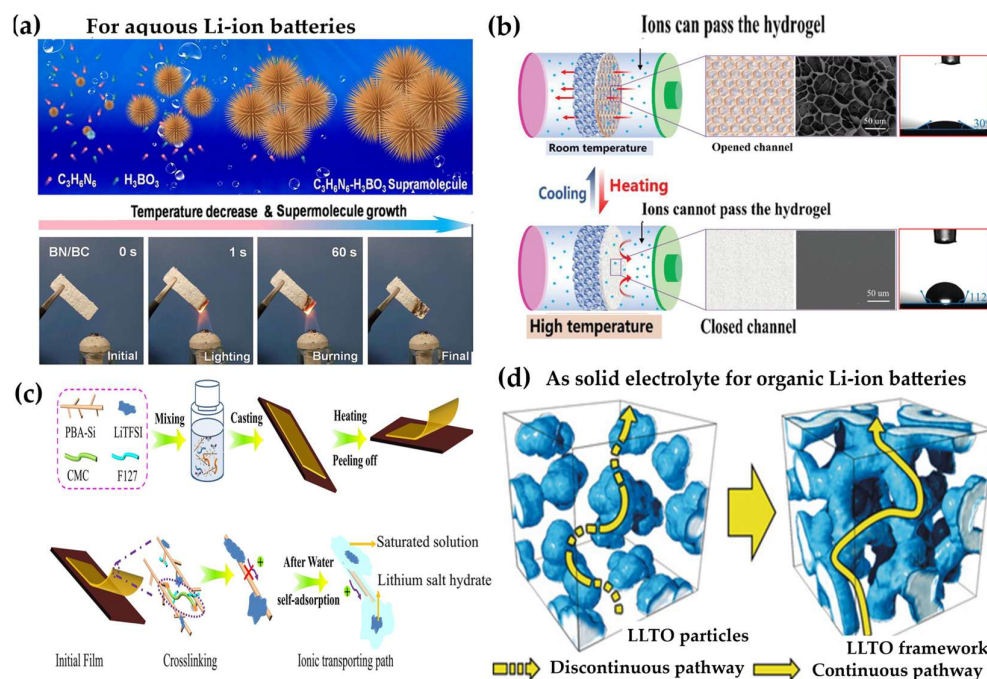


**Figure 9.** Schematics illustrating various hydrogel-based electrolyte systems developed for energy storage applications, emphasizing their structural configurations and functional contributions to ionic transport and mechanical stability. Panels (a–d) depict representative designs reported in recent literature. Adapted with permission from ref. [120,122], Elsevier; and ref. [121,123], Wiley & Sons.

To improve high-temperature safety, thermos-responsive hydrogel separators were developed by polymerizing hydrogel layers on hydrophilic membranes. These smart separators block lithium-ion transport at elevated temperatures and reopen upon cooling. By adjusting lithium salt concentration (e.g.,  $1 \text{ M LiNO}_3$ ), the shut-off temperature was tunable between  $30\text{--}80^\circ\text{C}$  (Figure 9b). A self-protecting  $\text{LiMn}_2\text{O}_4$ /carbon-coated  $\text{LiTi}_2(\text{PO}_4)_3$  battery using this separator demonstrated stable operation in high-temperature environments [121].

Stretchable battery components have also been realized using crumpled-structured nanowires (NWs) and crosslinked hydrogels. These materials form interconnected wrinkled NWs and robust hydrogel interfaces that maintain electrochemical stability under strain. A fully stretchable LIB (FSSLIB) using this design achieved  $119 \text{ mAh g}^{-1}$  capacity and retained 91.6% of its capacity after 250 stretching cycles at 100% strain [124].

Incorporating self-healing into stretchable systems, freestanding hydrogel electrolyte films (HEFs) were fabricated using hygroscopic lithium salts and dynamic polymer networks (PBA-Si, CMC, F127, and LiTFSI). These HEFs (Figure 9c) absorbed ambient moisture to form ionic pathways,



exhibited  $1.15 \text{ mS cm}^{-1}$  conductivity, and stretched up to 300% of their original length. A full cell using HEF with NTCDA and  $\text{LiMn}_2\text{O}_4$  retained 73.2% capacity after 1,000 cycles at  $1 \text{ A g}^{-1}$ , demonstrating excellent mechanical and electrochemical performance for wearable applications [122].

Beyond soft materials, hydrogels have been used as templates for solid-state frameworks. A 3D nanostructured  $\text{Li}_{0.35}\text{La}_{0.55}\text{TiO}_3$  (LLTO) framework derived from hydrogel precursors (Figure 9d) significantly improved Li-ion conductivity ( $8.8 \times 10^{-5} \text{ S cm}^{-1}$  at room temperature), serving as a nanofiller in composite polymer electrolytes. Similarly, Bae et al. [123] used nanostructured hydrogels to fabricate 3D interconnected garnet frameworks of  $\text{Li}_{6.28}\text{La}_3\text{Zr}_2\text{Al}_{0.24}\text{O}_{12}$  (LLZO), achieving high conductivity ( $\sim 10^{-3} \text{ S cm}^{-1}$  at  $60^\circ\text{C}$ ) and excellent interfacial stability with lithium metal.

These advancements highlight the versatility of hydrogel-based materials in addressing the mechanical, thermal, and electrochemical challenges of next-generation lithium-ion batteries, particularly for flexible, wearable, and high-safety applications.

### 3.2.4. Hydrogels Under Extreme Conditions

Hydrogels are increasingly used in battery systems due to their excellent ionic conductivity, mechanical flexibility, and compatibility with aqueous environments. However, their performance under extreme conditions—such as low temperatures, dehydration, and narrow electrochemical stability windows—poses significant challenges that limit their broader application in high-performance energy storage systems.

One of the primary limitations is the behavior of water within hydrogel matrices. At temperatures below  $0^\circ\text{C}$ , water in the electrolyte freezes, drastically reducing solvating ability and ionic mobility. This leads to salt crystallization and loss of structural flexibility, severely impairing battery performance. The freezing behavior is governed by the interaction energy between water molecules ( $E_{\text{ww}} \approx -5.75 \text{ kcal mol}^{-1}$ ). In conventional PVA hydrogels, the polymer–water interaction energy ( $E_{\text{pw}} \approx -6.11 \text{ kcal mol}^{-1}$ ) is only marginally stronger, which is insufficient to prevent freezing. In contrast, PAA hydrogels, due to their highly polarized carboxylic groups ( $-\text{COOH}$ ), exhibit a much stronger interaction with water ( $E_{\text{pw}} \approx -12.92 \text{ kcal mol}^{-1}$ ), effectively disrupting ice formation. As a result, PAA-based hydrogel electrolytes maintain high conductivity ( $20 \times 10^{-2} \text{ S cm}^{-1}$ ) even at  $-20^\circ\text{C}$  (Figure 10a–b) [125].

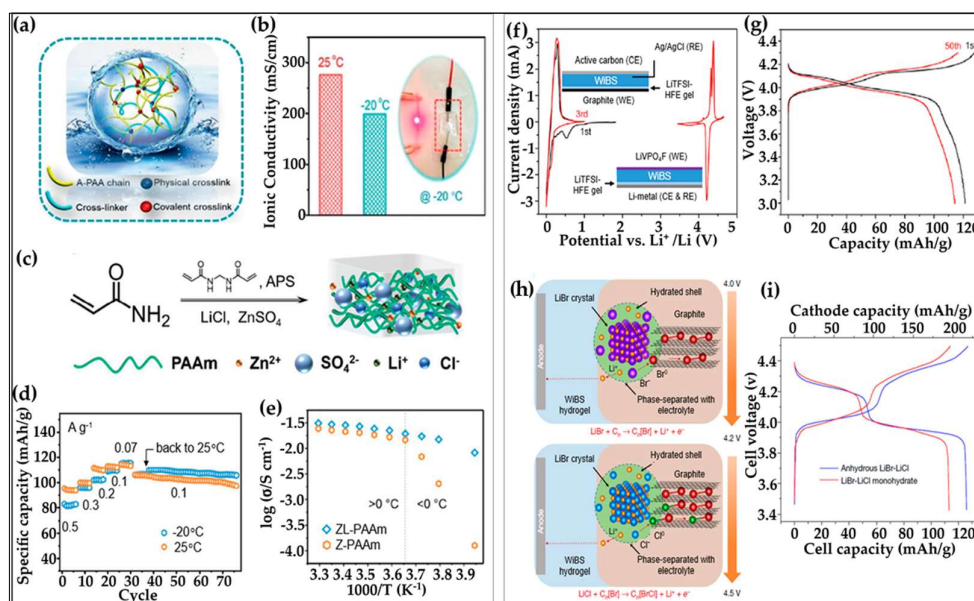


**Figure 10.** Schematics and experimental data illustrating the design and performance of hydrogel-based electrolytes under varying temperature conditions. (a, b) Structure and ionic conductivity of KOH-filled A-PAA hydrogel, including its functionality at  $-20\text{ }^{\circ}\text{C}$ , adapted with permission from ref. [125], Wiley & Sons. (c–e) Synthesis and electrochemical behavior of ZL-PAAm hydrogel, highlighting rate capability and temperature-dependent conductivity, adapted with permission from ref. [126], Wiley & Sons. (f, g) Electrochemical characterization of LiTFSI-HFE gel-coated electrodes in hydrogel-WiBS systems, including cyclic voltammetry and voltage profiles, adapted with permission from ref. [84], Elsevier. (h, i) Conversion–intercalation mechanism and voltage profiles of LBC-G composite cathodes in WiBS-based full cells with different lithium salt hydrates, adapted with permission from ref. [127], Springer Nature.

To further enhance low-temperature performance, Zhu et al. [126] developed a dual-salt hydrogel system by incorporating 2 M  $\text{ZnSO}_4$  and 4 M  $\text{LiCl}$  into a PAAm matrix (ZL-PAAm). The synergistic effect of strongly hydrated ions ( $\text{Zn}^{2+}$  and  $\text{SO}_4^{2-}$ ) and electrostatic stabilization from  $\text{Li}^+$  and  $\text{Cl}^-$  ions reduced water crystallization. This enabled  $\text{Zn/LiFePO}_4$  batteries to perform reliably at  $-20\text{ }^{\circ}\text{C}$ , with electrochemical characteristics comparable to those at room temperature (Figure 10c–e).

Another major challenge is dehydration, especially under ambient or elevated temperatures. Water's high vapor pressure (4.25 kPa at  $30\text{ }^{\circ}\text{C}$ ) makes hydrogel electrolytes prone to drying out, unlike organic solvents such as ethylene carbonate (7.8 Pa). Bai et al. [287] addressed this by incorporating hygroscopic salts like 12 M  $\text{LiCl}$  into PAAm hydrogels, which formed a tightly bound solvation sheath around water molecules, significantly reducing evaporation. Similarly, bisalt aqueous electrolytes demonstrated improved dehydration resistance, with hydrate melts showing vapor pressures as low as 0.5 kPa [128]. Additional strategies include coating hydrogels with elastomeric layers to retain moisture [129–131].

Hydrogels also face limitations due to their narrow electrochemical stability window ( $\sim 1.23\text{ V}$ ), which restricts their use in high-voltage lithium-ion batteries. While “water-in-salt” electrolytes (e.g., 21 M LiTFSI) can extend this window to  $\sim 3.0\text{ V}$  [132], they remain incompatible with typical anode materials like Li metal, graphite, and silicon due to cathodic instability. To overcome this, researchers have developed protective strategies such as coating anodes with highly fluorinated ether (HFE) gels to form stable solid electrolyte interphases (SEIs). This allows hydrogel electrolytes to operate with conventional Li-ion electrodes. For instance, WiBS electrolytes gelled in PVA or PEO showed stable redox behavior with graphite and  $\text{LiVPO}_4\text{F}$  electrodes (Figure 10f–g) [84].

Yang et al. [127] further demonstrated a high-voltage aqueous battery using WiBS–PEO hydrogel with a graphite anode and a  $(\text{LiBr})_{0.5}\text{--}(\text{LiCl})_{0.5}$ –graphite (LBC-G) cathode, achieving  $\sim 120\text{ mAh g}^{-1}$  capacity and  $\sim 4\text{ V}$  operating voltage (Figure 10h–i).

These studies collectively demonstrate that through strategic material engineering—such as salt selection, polymer backbone design, and interface protection—hydrogels can be adapted to function effectively under extreme conditions. Understanding the molecular interactions between water, ions, and polymer chains is essential for designing robust hydrogel electrolytes for next-generation energy storage technologies.

### 3.3. Hydrogels for Sodium-Ion Batteries

Sodium-ion batteries (NIBs) have gained attention as a promising alternative to lithium-ion batteries due to sodium's natural abundance, low cost, environmental sustainability, and suitable redox potential ( $E^{\circ} \text{Na}^+/\text{Na} = -2.71\text{ V}$ ) [209,210]. With a theoretical energy density of  $1165\text{ Wh kg}^{-1}$ , NIBs are well-suited for large-scale energy storage and decarbonization efforts [133–135].

Despite these advantages, NIBs face several challenges that hinder their practical deployment. These include low energy density, poor cycling stability, limited low-temperature tolerance, and water-induced parasitic reactions. A major issue is the large ionic radius of  $\text{Na}^+$ , which complicates fast ion diffusion and leads to structural degradation and volume changes in electrode materials during cycling. This results in poor reversibility and dissolution of active materials, especially in anodes, reducing their electrochemical contribution [136].

Hydrogels offer a versatile solution to these problems. Their crosslinked polymer networks retain water and improve mechanical and electrochemical stability [137]. The porous structure of hydrogels accommodates volume expansion and facilitates rapid  $\text{Na}^+$  transport during insertion/extraction [138]. Additionally, hydrogels exhibit excellent stretchability and ionic conductivity, making them suitable for electrolyte modification and enhancing compatibility with electrodes. Their responsiveness to stimuli also enables the design of self-adaptive structures for low-temperature operation [139].

Hydrogels are non-toxic, low-cost, and easily modifiable, supporting the development of safer and more sustainable NIBs. Recent designs have incorporated hydrogels to improve thermal stability, mechanical flexibility, and interface contact, while also suppressing electrolyte leakage. In these systems, hydrogels have been applied as electrolytes [137,139,140], anode materials [141], and templates for cathodes [136,138], as illustrated in Figure 11(a–d).

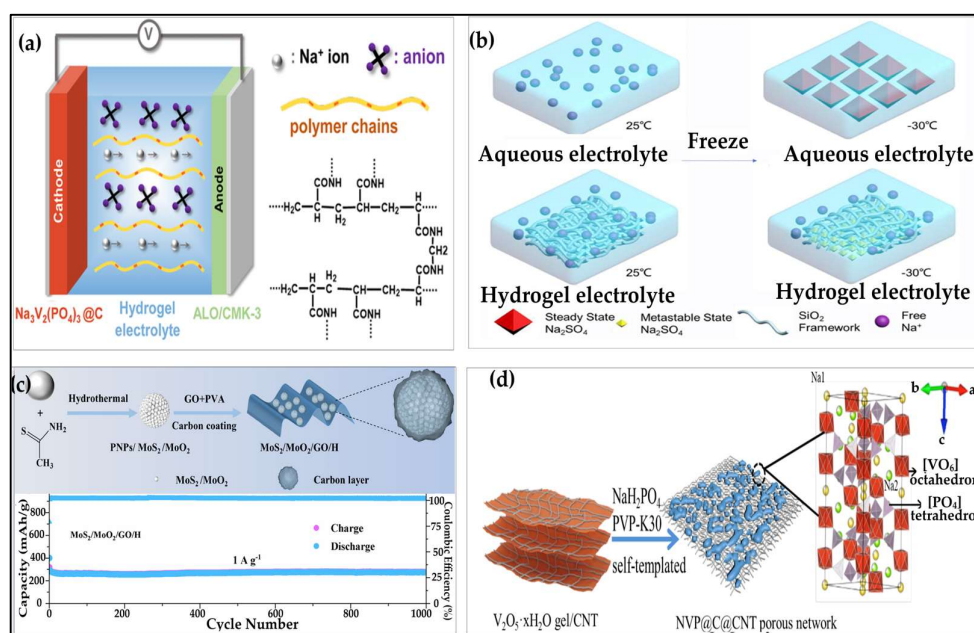


**Figure 11.** Representative schematics and performance data highlighting the application of hydrogel-based electrolytes in sodium-ion batteries (NIBs). (a) Configuration of an NIB employing a polyacrylamide hydrogel electrolyte with ALO/CMK-3 anode and NVP@C cathode, adapted with permission from ref. [137], copyright© 2018 American Chemical Society. (b) Comparison of freezing behavior between aqueous  $\text{Na}_2\text{SO}_4$  and  $\text{Na}_2\text{SO}_4$ - $\text{SiO}_2$  hydrogel electrolytes from 25 °C to -30 °C, adapted with permission from ref. [139], Elsevier. (c) Preparation and long-term cycling performance of  $\text{MoS}_2/\text{MoO}_2/\text{GO}/\text{H}$  composite anode, adapted with permission from ref. [141], Elsevier. (d) Synthesis schematic of  $\text{Na}_3\text{V}_2(\text{PO}_4)_3@\text{CNT}$  composite cathode, adapted with permission from ref. [138], Elsevier.

### 3.3.1. Hydrogel Electrolytes for Sodium-Ion Batteries

To address the low-temperature limitations of sodium-ion batteries (NIBs), Cheng et al. [139] developed a  $\text{Na}_2\text{SO}_4$ - $\text{SiO}_2$  hydrogel electrolyte using fumed silica,  $\text{Na}_2\text{SO}_4$ , and methyl alcohol (Figure 11b). This design leverages the strong polarity of  $\text{Na}_2\text{SO}_4$  and the anti-freezing properties of methyl alcohol to suppress salt precipitation and maintain ionic conductivity at sub-zero temperatures. The hydrogel forms stable Si-O-Si bridges and hydrogen bonds, enabling a conductivity of  $0.070 \text{ mS cm}^{-1}$  at -30 °C. The resulting NIB delivered reversible capacities of  $78.9 \text{ mAh g}^{-1}$  at -20 °C and  $61.8 \text{ mAh g}^{-1}$  at -30 °C, demonstrating excellent low-temperature performance. Zhong et al. [137] tackled the issue of anode dissolution by pairing an organic alloxazine (ALO) anode with a conductive carbon material (CMK-3) and a polyacrylamide hydrogel electrolyte (Figure 11a).

The hydrogel preserved water content and stabilized the interface, while CMK-3 enhanced conductivity and reduced ALO dissolution. The optimized system achieved a high capacity of 160 mAh g<sup>-1</sup>, an average discharge voltage of 1.03 V, and an energy density of 50 Wh kg<sup>-1</sup>, with 90% capacity retention after 100 cycles at 2 C and 146 mAh g<sup>-1</sup> at 10 C.

### 3.3.2. Hydrogel Anodes for Sodium-Ion Batteries

To improve anode performance and cycling stability, Zhang et al. [141] developed a 3D MoS<sub>2</sub>/MoO<sub>2</sub>/graphene oxide/polyvinyl alcohol hydrogel composite using a cationic absorption method, hydrothermal synthesis, and gelation (Figure 11c). MoS<sub>2</sub> offers high capacity and a layered structure but suffers from poor conductivity and volume expansion. MoO<sub>2</sub> was introduced to form a stable heterojunction, while graphene oxide provided mechanical strength and conductivity. The resulting hydrogel composite formed a highly conductive, ultrathin carbon network with excellent electrochemical kinetics. The anode delivered 350 mAh g<sup>-1</sup> after 100 cycles at 0.1 A g<sup>-1</sup> and 273 mAh g<sup>-1</sup> after 1000 cycles at 1 A g<sup>-1</sup>, demonstrating outstanding long-term cycling stability and minimal capacity decay.

### 3.3.3. Hydrogel Cathodes for Sodium-Ion Batteries

To improve the performance and cycling stability of sodium-ion battery (NIB) cathodes, researchers have explored hydrogel-based porous network designs and surface engineering strategies. These approaches aim to address challenges such as limited ion transport, poor conductivity, and structural degradation during cycling. Yan et al. [138] developed a hydrogel self-templated method to fabricate a 2D porous Na<sub>3</sub>V<sub>2</sub>(PO<sub>4</sub>)<sub>3</sub>@C@CNT (NVP) cathode structure (Figure 11d). The design integrates 0D carbon-coated Na<sub>3</sub>V<sub>2</sub>(PO<sub>4</sub>)<sub>3</sub> nanoparticles with 1D carbon nanotubes (CNTs), forming a conductive and open network that facilitates rapid Na<sup>+</sup> diffusion and accommodates volume changes. The carbon coating enhances electronic conductivity and interparticle contact, while the porous architecture supports long-term structural integrity. As a result, the NVP cathode exhibits exceptional cycling stability—retaining 94% of its capacity after 4500 cycles at 5 C—and delivers a high rate capability of 84 mAh g<sup>-1</sup> at 10 C. Complementing this, Cheng et al. [136] synthesized a 3D porous Na<sub>3</sub>V<sub>2</sub>(PO<sub>4</sub>)<sub>3</sub>/C cathode using hydrogel and hydrothermal methods. The resulting particles (100–200 nm) offer high surface area and conductivity. This cathode achieved a specific capacity of 62.1 mAh g<sup>-1</sup> at 10 C, with 98% retention after 140 cycles at 1 C. Even after 2000 cycles at 5 C, the capacity remained at 80.4 mAh g<sup>-1</sup>, with 86% retention.

These studies demonstrate the effectiveness of hydrogel-based cathode designs in enhancing the electrochemical performance, rate capability, and long-term durability of NIBs, paving the way for more robust and scalable energy storage technologies.

### 3.4. Hydrogel Electrolytes for Zinc-Ion Battery

Hydrogel electrolytes have emerged as a promising solution to address key challenges in zinc-ion batteries (ZIBs), which are increasingly favored for their safety, affordability, and environmental compatibility [142,143]. Despite these advantages, ZIBs face significant limitations, including zinc dendrite formation, side reactions, and a narrow electrochemical stability window due to water decomposition. Dendrites, which form through uneven Zn<sup>2+</sup> deposition during cycling, can penetrate the separator and cause internal short circuits, posing serious safety risks [144]. The probability of such failures increases under high current densities and is exacerbated by surface defects and polarization effects. Additionally, side reactions at the electrode–electrolyte interface consume active materials and generate gases such as H<sub>2</sub> and O<sub>2</sub>, leading to capacity loss and reduced Coulombic efficiency [145,146]. As illustrated in Figure 12a, [144] dendrite nucleation and growth are governed by epitaxial and spiral dislocation mechanisms, influenced by factors such as surface tension and temperature gradients [147,148]. Hydrogel electrolytes mitigate these issues through their interconnected porous networks that facilitate uniform ion transport [149], functional groups (–OH,



–COOH, –NH<sub>2</sub>) that coordinate with Zn<sup>2+</sup> to suppress hydrogen evolution [30], and mechanical robustness that restrains dendrite growth. Moreover, their self-healing properties and thermal stability enhance long-term performance and enable operation under extreme conditions. By stabilizing the electrode interface and extending the voltage window, hydrogels significantly improve the safety, cycling life, and energy density of ZIBs, making them a critical component in the advancement of next-generation aqueous battery technologies.

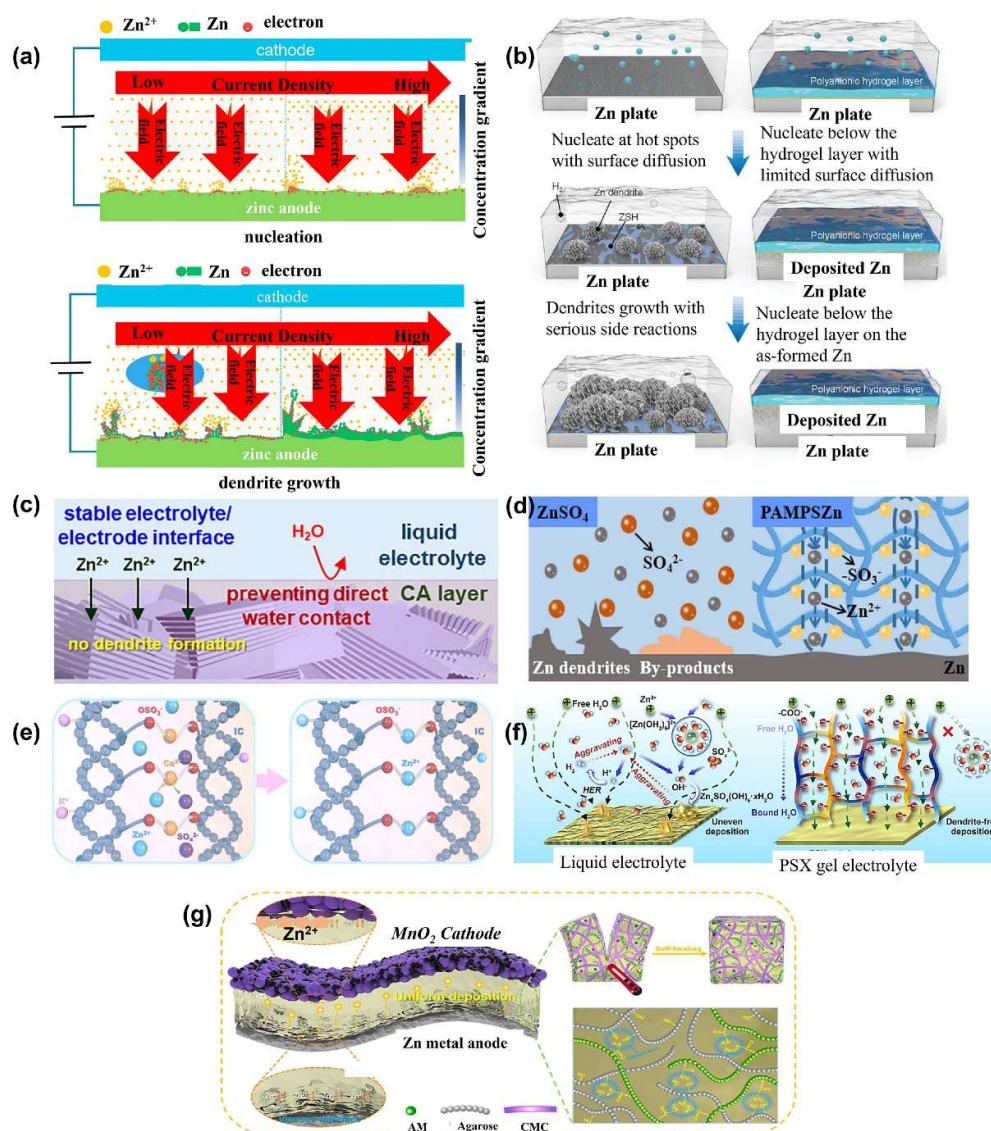


**Figure 12.** Schematics and illustrations highlighting recent strategies to address zinc dendrite formation and enhance electrolyte stability in zinc-based batteries. (a) Mechanistic depiction of zinc dendrite growth, redrawn & reproduced with permission [144], Elsevier. (b) comparison of Zn deposition behavior on bare Zn and Zn–SHn surfaces, redrawn & reproduced with permission [150], Wiley & Sons. (c) influence of stable electrolyte formulations on dendrite suppression, reproduced with permission from ref. [151], Elsevier. (d) polymer chains containing –SO<sub>3</sub><sup>–</sup> groups to regulate Zn<sup>2+</sup> migration, reproduced with permission from ref. [152], Elsevier. (e) design of single zinc-ion conducting hydrogel electrolytes, reproduced with permission [153], copyright© 2021 American Chemical Society.; (f) self-healing hydrogel electrolyte systems, reproduced with permission from ref. [154], Elsevier; and (g) hydrogel networks incorporating polymeric anions for improved ion transport and structural integrity, reproduced with permission from ref. [155], Elsevier.



To overcome the electrochemical and mechanical limitations of zinc-ion batteries (ZIBs), researchers have developed multifunctional hydrogel electrolytes with tailored properties that enhance performance, safety, and longevity. Key design strategies include engineering compatible electrode–electrolyte interfaces, incorporating additives such as plasticizers and metal ions, and introducing anionic chains to regulate  $\text{Zn}^{2+}$  transport [151,152,156–158]. These approaches have led to the development of hydrogels with enhanced mechanical strength, thermal stability, and self-healing capabilities, which effectively suppress dendrite growth and mitigate side reactions. For instance, Yang et al. [150,151] designed a zincophilic polyanionic hydrogel chemically bonded to the Zn anode via O–Zn linkages, improving interfacial adhesion and suppressing hydrogen evolution (Figure 12b). Park et al. utilized a natural polysaccharide-based hydrogel to form a biocompatible barrier that reduced corrosion and enabled long-term cycling (Figure 12c). Functional composites such as PAM/phosphonated graphene oxide [156], Na-montmorillonite/PAM hybrids [157], and dual-network PAMPS/PAM hydrogels [158] have demonstrated improved ionic conductivity and mechanical integrity. Anion chain-directed strategies further enhance  $\text{Zn}^{2+}$  transport, as shown by polyanionic hydrogels [158], polyzwitterionic systems [159], and single-ion electrolytes like P(ICZn-Aam) [153]. Cong et al. [152] synthesized a polyanionic hydrogel via ion exchange and radical polymerization, guiding  $\text{Zn}^{2+}$  along confined pathways and reducing side reactions (Figure 12d). Chan et al. [153] developed a single-ion  $\text{Zn}^{2+}$  hydrogel electrolyte (P(ICZn-Aam)) using iota carrageenan and acrylamide. The  $\text{SO}_3^{2-}$  groups facilitate  $\text{Zn}^{2+}$  migration along the polymer chain, enhancing ion transport and interfacial stability, leading to improved Zn deposition and cycling performance (Figure 12e). Fu et al. [154] achieved high ionic conductivity and  $\text{Zn}^{2+}$  migration number using a PVA–xanthan gum hydrogel (Figure 12f). Ling et al. [155] incorporated carboxymethyl cellulose (CMC) into agarose and polyacrylamide (PAM) networks, forming a porous, hydrophilic structure. This enhanced ionic conductivity, achieving  $23.1 \text{ mS}\cdot\text{cm}^{-1}$  at  $25^\circ\text{C}$  (Figure 12g). Collectively, these innovations in hydrogel design offer a versatile platform for addressing dendrite formation and side reactions, paving the way for high-performance, durable ZIBs.

### 3.4.1. High-Voltage Hydrogel-Based Zinc-Ion Batteries

Achieving high operating voltage in zinc-ion batteries (ZIBs) is crucial for enhancing energy density and meeting the demands of advanced energy storage systems. However, aqueous ZIBs are inherently limited by parasitic reactions such as hydrogen evolution (HER) and oxygen evolution (OER), triggered by water decomposition beyond its electrochemical stability window ( $\sim 1.23 \text{ V}$ ). These side reactions reduce Coulombic efficiency, accelerate electrode degradation, and promote dendrite formation. To address these challenges, researchers have employed strategies including reducing free water content, introducing highly concentrated zinc salts, incorporating anion chains for guided ion transport, and engineering stable electrode–electrolyte interfaces [160–163]. Hydrogel electrolytes have proven effective in this context due to their ability to bind water molecules and suppress side reactions, enabling stable high-voltage operation.

For example, Wang et al. [162] developed a water-poor polyzwitterionic hydrogel with  $-\text{SO}_3^{2-}$  and  $-\text{C}_3\text{N}^+$  groups, achieving a voltage window exceeding  $2 \text{ V}$  and ionic conductivity of  $2.6 \times 10^{-3} \text{ S cm}^{-1}$  (Figure 13a). Xu et al. [161] developed a cellulose-based hydrogel electrolyte with a dense structure and strong mechanical integrity (Figure 13b). This design suppresses dendrite growth and minimizes free water content, reducing side reactions at high voltage. As a result, it enables stable, high-power energy storage under elevated voltage and current conditions.

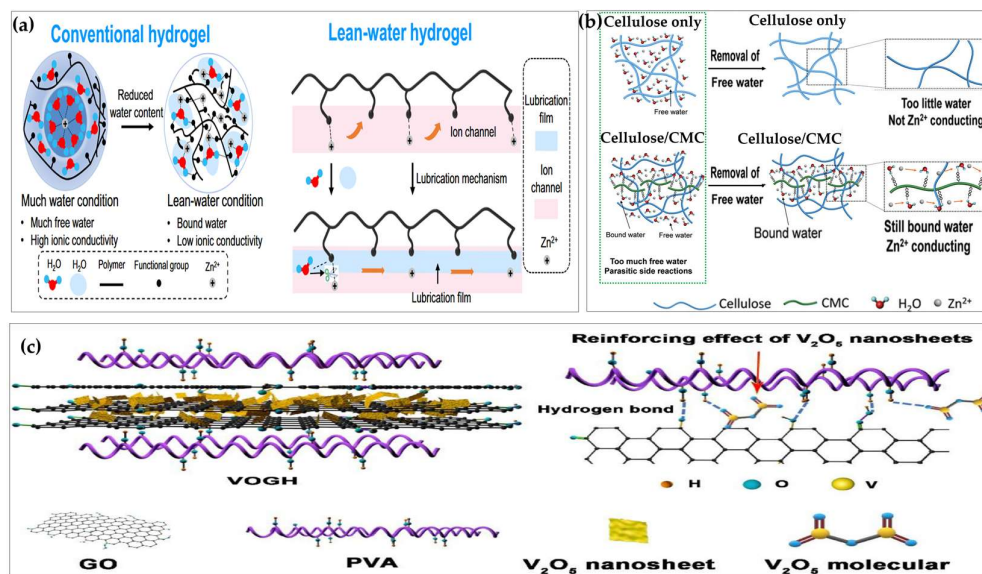


**Figure 13.** Schematics illustrating advanced electrolyte strategies in zinc-ion batteries: (a) lean-water electrolyte systems designed to minimize side reactions [162]; (b) bound-water electrolytes enhancing stability under low-temperature conditions [161]; and (c) engineered interfaces promoting hydrogen bonding between the electrolyte and electrode for improved compatibility and performance, adapted with permission from ref. [164], Elsevier.

Interface engineering has also played a vital role, as demonstrated by Ma et al. [163] using sol-gel modified hydrogels with Prussian Blue cathodes, and by Wu et al. [108] and Lv et al. [164] employing freeze–thaw cycles to enhance hydrogen bonding and interfacial stability (Figure 13c).

Xu et al. [160] and Li et al. [165] fabricated cellulose-based hydrogels with bound water and strong hydrogen bonding, achieving voltage windows up to 1.9 V and energy densities of 255.4 Wh kg<sup>-1</sup>. Zhang et al. [166] and Lu et al. [167] introduced multi-crosslinked and biodegradable hydrogels, respectively, both demonstrating stable cycling and voltage ranges up to 2.0 V. Additional innovations include gelatin-based hydrogels [97], PVA-based systems doped with LiTFSI and ZnOTf<sub>2</sub> [98,168] (Figure 14a–c), and PVA–gelatin hydrogels with high ZnCl<sub>2</sub> concentration [169] (Figure 14d–e), all of which convert free water into bound water and suppress side reactions.

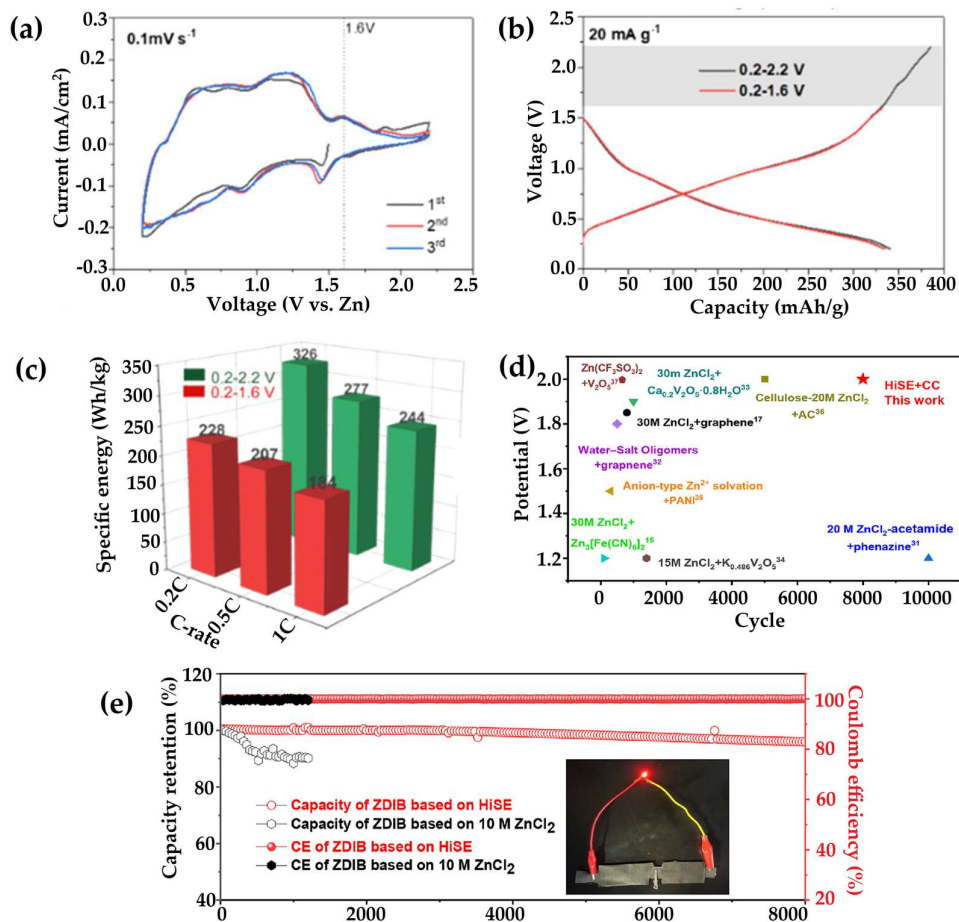


**Figure 14.** Electrochemical performance and voltage behavior of zinc-ion batteries using gel polymer and hydrogel-based electrolytes. (a) Cyclic voltammogram of Zn/V<sub>2</sub>O<sub>5</sub> cells with gel polymer aqueous electrolyte; (b) corresponding charge-discharge profiles; (c) specific energy across different voltage windows, adapted with permission [168] copyright© 2020 American Chemical Society. (d) Comparative analysis of potential windows for zinc-ion batteries with different electrolytes systems; (e) cycling stability of hydrogel water-in-salt electrolyte versus 10 M ZnCl<sub>2</sub> electrolyte, adapted with permission from ref. [169], Elsevier.

### 3.4.2. Self-Healing Hydrogel-Based Zn-Ion Batteries

In the context of wearable and flexible electronics, zinc-ion batteries (ZIBs) are frequently subjected to mechanical stress such as bending, twisting, and stretching, which can lead to electrolyte leakage, structural fracture, and diminished ionic conductivity. These mechanical deformations compromise electrochemical performance and pose safety risks, especially under repeated fatigue that disrupts the conductive network and shortens battery lifespan. To address these challenges, self-healing hydrogel electrolytes have been developed, leveraging dynamic and reversible interactions—including covalent and non-covalent bonding, ionic crosslinking, hydrogen bonding, and host-guest interactions—to autonomously restore mechanical integrity and electrochemical functionality [170,171]. Huang et al. [172] demonstrated a PVA/Zn(TFSI)<sub>2</sub> hydrogel fabricated via freeze-thaw cycles, where -OH groups enabled hydrogen bonding and self-healing after multiple cuts (Figure 15a-b).

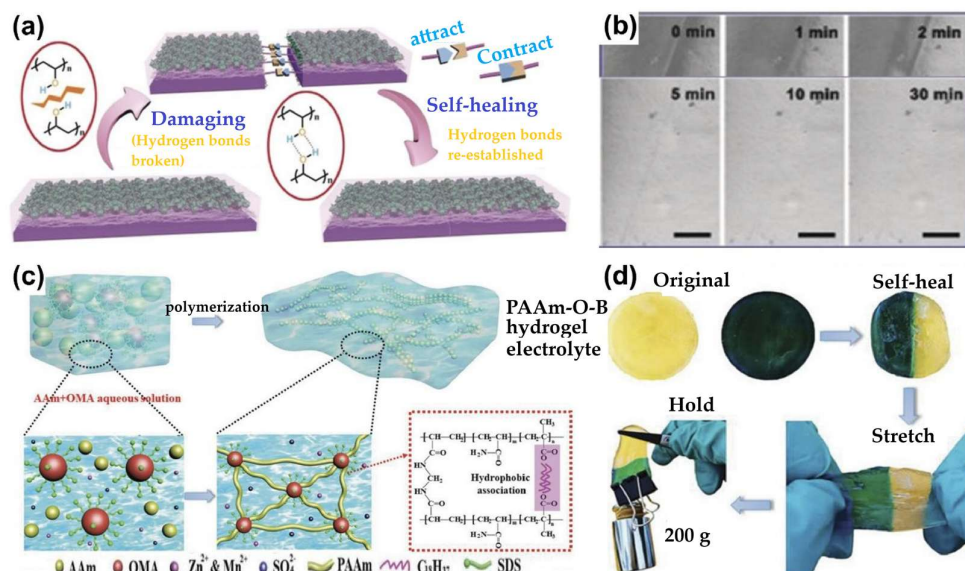


**Figure 15.** Schematics and visual demonstrations of self-healing hydrogel electrolytes in zinc-ion batteries. (a, b) Design and healing behavior of an integrated all-in-one self-healing ZIB system, redrawn and reproduced with permission [172], Wiley & Sons; (c) synthesis pathway and (d) self-repairing capability of PAAM-O-B hydrogel electrolyte, adapted with permission [173], Wiley & Sons.

Liu et al. [174] constructed a flexible ZIB using  $\text{VS}_2$  nanosheets and Zn nanowires with a PVA-based self-healing electrolyte, achieving high capacity and mechanical resilience. Li et al. [175] introduced a  $\text{COO}-\text{Fe}$ -modified PVA hydrogel in a quasi-solid-state Zn/MnO<sub>2</sub> battery, which not only self-healed but also suppressed dendrite growth and side reactions. Liu et al. [176] incorporated Hbimcp into PPO chains, forming  $\text{Zn}^{2+}$ -ligand complexes with reversible coordination bonds that enabled dynamic repair and high ionic conductivity. Additional innovations include zinc alginate hydrogels with carboxylate groups [177], double-crosslinked PAM hydrogels capable of enduring 50 fracture/healing cycles [173] (Figure 15c–d), and PAM-based Zn/Mn-doped hydrogels fabricated via photoinitiated polymerization [178]. Liu et al. [179] enhanced safety and reversibility using  $\text{Zn}^{2+}$ -induced supramolecular interactions in chitosan/PAM hydrogels. To further improve mechanical strength, Shen et al. [180] embedded halloysite nanotubes (HNTs) into PAM networks, resulting in superior dissipation and hydrogen bonding. These self-healing hydrogel systems collectively offer robust mechanical adaptability and electrochemical stability, making them ideal for next-generation flexible and wearable ZIB applications.

### 3.5. Hydrogels for Magnesium-Ion Batteries

Magnesium-ion batteries (MIBs) are gaining attention as sustainable alternatives to lithium-ion batteries due to magnesium's abundance, low cost, non-toxicity, high volumetric capacity ( $3833 \text{ mAh cm}^{-3}$ ), and dendrite-free cycling [181–183]. Magnesium is also lightweight ( $1.74 \text{ g cm}^{-3}$ ) and stable in ambient conditions, making it suitable for use as a pure metal anode.

However, MIBs face several challenges that hinder their practical deployment. The primary issue lies in the incompatibility between magnesium anodes and conventional electrolytes. Magnesium readily forms a passivation layer in contact with common solvents (e.g., esters, carbonates, nitriles) and contaminants (e.g., water,  $\text{CO}_2$ ), which blocks  $\text{Mg}^{2+}$  transport and impairs reversibility [184]. Additionally, MIBs suffer from limited oxidative stability, sluggish  $\text{Mg}^{2+}$  diffusion in cathodes due to strong electrostatic interactions, and insufficient energy density and cycle life [184,185].



To address these limitations, research has focused on optimizing MIB components— anodes, cathodes, electrolytes, and interfacial materials [184–186]. Hydrogels have emerged as promising candidates due to their tunable structure, low toxicity, and ability to support  $\text{Mg}^{2+}$  mobility. Their porous networks and stimuli-responsive properties can enhance ionic conductivity and suppress uneven Mg deposition, even under extreme conditions [187–189].

### 3.5.1. Hydrogels as Electrolyte for MIBs

Despite their potential, hydrogel applications in MIBs remain in early stages. Yang et al. [188] pioneered the use of hydrogels as electrolytes for MIBs (Figure 16A), targeting performance degradation at sub-zero temperatures. They introduced an unconventional deep eutectic solvent (DES)-based hydrogel using polyacrylamide (PAAm) and  $\text{MgCl}_2$ . Unlike conventional DESs, which suffer from high viscosity and low conductivity at low temperatures, the  $\text{MgCl}_2$ -based DES disrupts hydrogen bonding among water molecules, lowering the freezing point and enhancing ionic mobility. The resulting PAAm/ $\text{MgCl}_2$  hydrogel electrolyte demonstrated exceptional anti-freezing properties (freezing point:  $-62\text{ }^\circ\text{C}$ ) and high ionic conductivity ( $2.77\text{ mS cm}^{-1}$  at  $-50\text{ }^\circ\text{C}$ ). The assembled quasi-solid-state MIB exhibited stable electrochemical performance across a wide temperature range ( $+25$  to  $-50\text{ }^\circ\text{C}$ ), with a discharge capacity of  $97.9\text{ mAh g}^{-1}$  at  $0.1\text{ A g}^{-1}$  and a high cycling stability of 1000 cycles. It retained 28% of its specific capacity at  $3\text{ A g}^{-1}$ , confirming its robustness under harsh conditions.

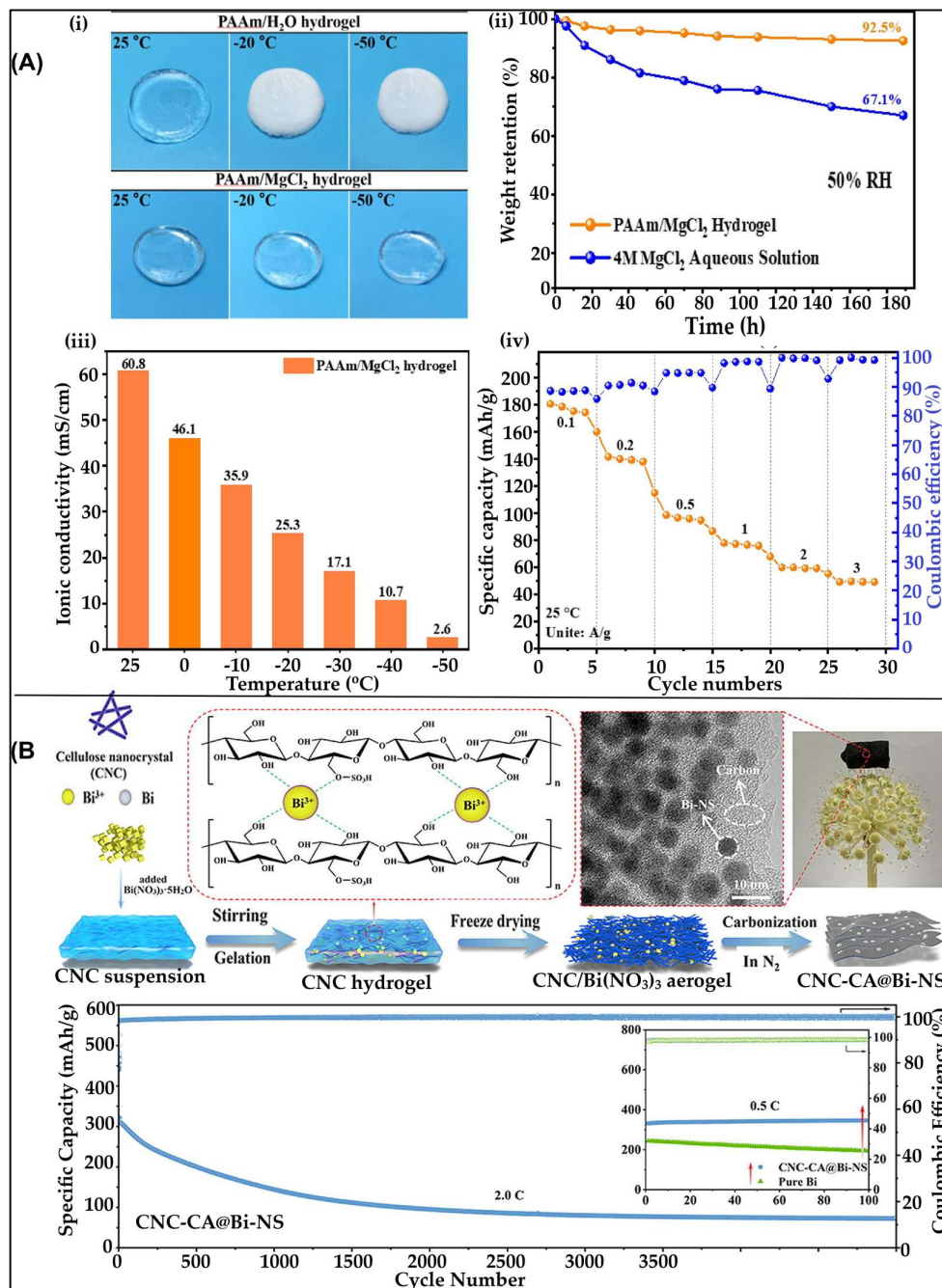


**Figure 16.** Multifunctional roles of hydrogels in magnesium-ion batteries (MIBs). (A) As electrolytes: (i) photographs of PAAm/H<sub>2</sub>O and PAAm/MgCl<sub>2</sub> hydrogel electrolytes at various temperatures (25 °C, -20 °C, -50 °C); (ii) mass change under 50% relative humidity at room temperature; (iii) ionic conductivity across a temperature range from -50 °C to +25 °C; and (iv) specific capacity of quasi-solid-state MIBs at 25 °C. (B) As anodes: (a) schematic of CNC-CA@Bi-NS fabrication process and (b) long-term cycling performance at 2.0 C over 5000 cycles. Adapted with permission from references [188,189], Elsevier.

### 3.5.2. Hydrogel-Derived Anodes for MIBs

To develop high-performance anodes for MIBs, Cheng et al. [189] proposed a strategy to mitigate the mechanical and structural degradation typically caused by volume fluctuations during magnesiumiation/demagnesiumiation. These fluctuations often lead to agglomeration and pulverization of the anode material, compromising battery performance. To address this, the researchers

encapsulated bismuth (Bi) nanoparticles within a cellulose nanocrystal (CNC) hydrogel-derived carbon aerogel matrix. The carbon substrate acts as a mechanical buffer, accommodating volume changes, while its 3D porous structure facilitates efficient electron and ion transport. Moreover, the uniform dispersion of Bi nanoparticles within the carbon network prevents agglomeration and enhances structural integrity.

For the first time, Cheng et al.[189] fabricated a Bi nanosphere/CNC hydrogel-derived carbon aerogel hybrid anode, denoted as CNC-CA@Bi-NS (Figure 16B). The synthesis involved ion-induced gelation and in-situ thermal reduction. Microcrystalline cellulose and bismuth nitrate pentahydrate were used to form CNC/Bi(NO<sub>3</sub>)<sub>3</sub> hydrogels, which were freeze-dried into aerogels and subsequently pyrolyzed to yield the final CNC-CA@Bi-NS material. The resulting anode demonstrated a high reversible capacity of 346 mAh g<sup>-1</sup> at 0.5 C after 100 cycles—approximately 90% of its theoretical capacity. It also exhibited excellent long-term cycling stability, maintaining 73 mAh g<sup>-1</sup> at 2 C over 5000 cycles with nearly 100% coulombic efficiency. These outstanding electrochemical properties are attributed to the homogeneous dispersion of Bi nanospheres, which mitigates agglomeration and volume expansion, and the conductive aerogel matrix, which enhances electrolyte accessibility and ion diffusion.

This design exemplifies how functional hydrogel-derived materials—such as anti-freezing electrolytes and structurally stable anodes—can significantly advance the performance and durability of MIBs and other next-generation energy storage systems.

### 3.6. Hydrogels for Aluminum-Ion Batteries

Aluminum-ion batteries (AIBs) have emerged as a compelling alternative to lithium-ion batteries due to aluminum's natural abundance, low cost, and safety profile. Aluminum offers a trivalent charge carrier (Al<sup>3+</sup>), which contributes to a high theoretical gravimetric capacity of 2980 mAh g<sup>-1</sup> and an exceptional volumetric capacity of 8040 mAh cm<sup>-3</sup>. AIBs typically consist of an Al-based anode, a cathode capable of hosting Al<sup>3+</sup> ions, an electrolyte, binder, and current collector. During discharge, Al atoms at the anode oxidize to release electrons and form Al<sup>3+</sup> ions, which migrate through the electrolyte to the cathode. The reverse occurs during charging.

AIBs are generally categorized into aqueous and non-aqueous systems based on the electrolyte solvent. Aqueous AIBs are environmentally friendly and cost-effective but face significant challenges: hydrogen evolution occurs before effective Al<sup>3+</sup> reduction, aluminum corrosion leads to passivating oxide films, and electrolyte decomposition impedes ion transport. Consequently, research has shifted toward non-aqueous AIBs, which offer better electrochemical stability, higher safety (non-volatility and non-flammability), and a broader electrochemical window.

Despite these advantages, AIBs still face fundamental limitations. The relatively high redox potential of aluminum (-1.66 V) compared to lithium (-3.04 V) and sodium (-2.71 V) results in a lower working voltage. Additionally, the trivalent nature of Al<sup>3+</sup> leads to sluggish ion kinetics, high overpotentials, and structural collapse of host materials during cycling [185,189,190]. Electrolyte leakage, unstable interfaces due to mechanical deformation, and poor separator compatibility further hinder performance. Moreover, many polymers effective in lithium-ion batteries fail in AIBs due to their inability to transport Al<sup>3+</sup> or their incompatibility with Lewis acidic ionic liquids used in non-aqueous systems.

Hydrogels have gained attention as potential electrolytes for AIBs due to their high ionic conductivity, chemical and thermal stability, non-toxicity, and low cost [191]. Their abundant functional groups can form strong interactions with Al<sup>3+</sup>, enhancing mechanical strength and crosslinking. However, hydrogel applications in AIBs are still in early development, and careful materials selection is crucial to ensure compatibility with aluminum chemistry.

#### 3.6.1. Hydrogels as Electrolytes for AIBs

To address the need for stable and aluminum-compatible electrolytes, Wang et al. [192] developed a thermoresponsive hydrogel electrolyte based on poly(N-isopropylacrylamide) (PNIPAM) (Figure 17).

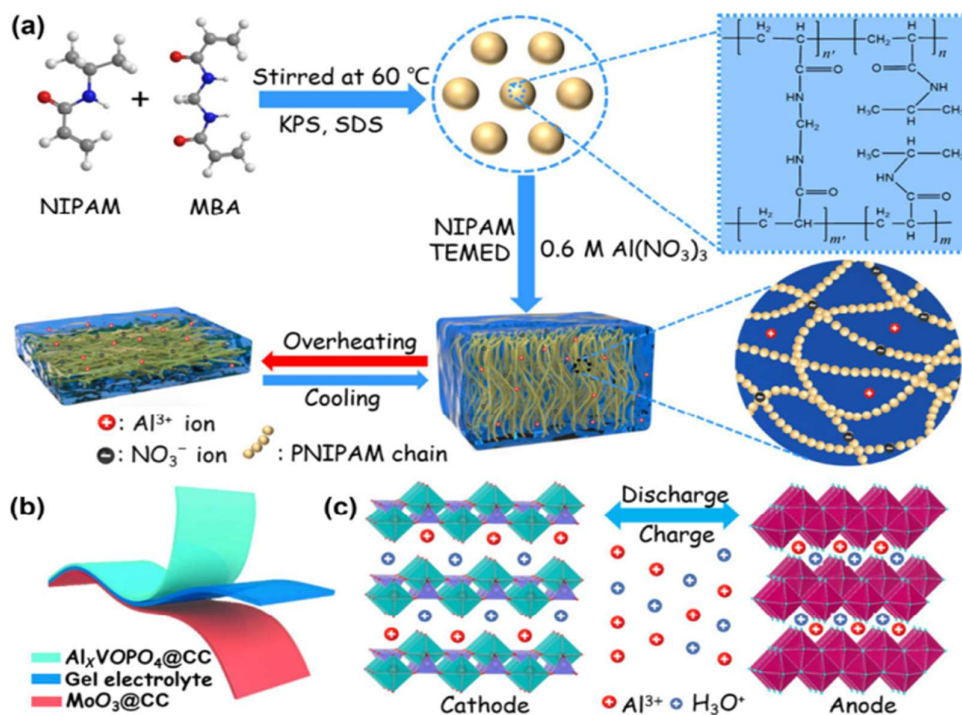


**Figure 17.** Design and functional integration of hydrogel-based smart electrolytes in hybrid ion batteries (HIBs). (a) Schematic of the synthesis route for PNIPAM hydrogel-based smart electrolyte; (b) configuration of a flexible aqueous HIB comprising Al<sub>x</sub>VOPO<sub>4</sub>·2H<sub>2</sub>O@carbon cloth cathode, PNIPAM hydrogel electrolyte, and MoO<sub>3</sub>@carbon cloth anode; (c) working principle of the HIB system based on intercalation-type electrodes, adapted with permission [192], Springer Nature.

Synthesized via free radical polymerization, PNIPAM features a balanced structure of hydrophilic amide (-CONH) and hydrophobic isopropyl (-CH(CH<sub>3</sub>)<sub>2</sub>) groups. At ambient temperature (24 °C), hydrogen bonding between water molecules and -CONH groups expands the hydrogel network, creating micropores that facilitate Al<sup>3+</sup> migration and enhance ionic conductivity (1.8 S/m). As temperature rises, the hydrogel network contracts due to weakened hydrogen bonds and strengthened hydrophobic interactions, reducing conductivity and preventing thermal runaway. The assembled battery – Al<sub>x</sub>VOPO<sub>4</sub>·2H<sub>2</sub>O cathode // PNIPAM hydrogel electrolyte // MoO<sub>3</sub> anode – exhibited a high specific capacity of 125 mAh g<sup>-1</sup> at 0.1 A g<sup>-1</sup> and remarkable cycling stability over 10,000 cycles at 2 A g<sup>-1</sup>, with no capacity fading.

In another study, Wang et al. [191] employed a gelatin–polyacrylamide hydrogel electrolyte to fabricate a safe and flexible AIB (Figure 18).



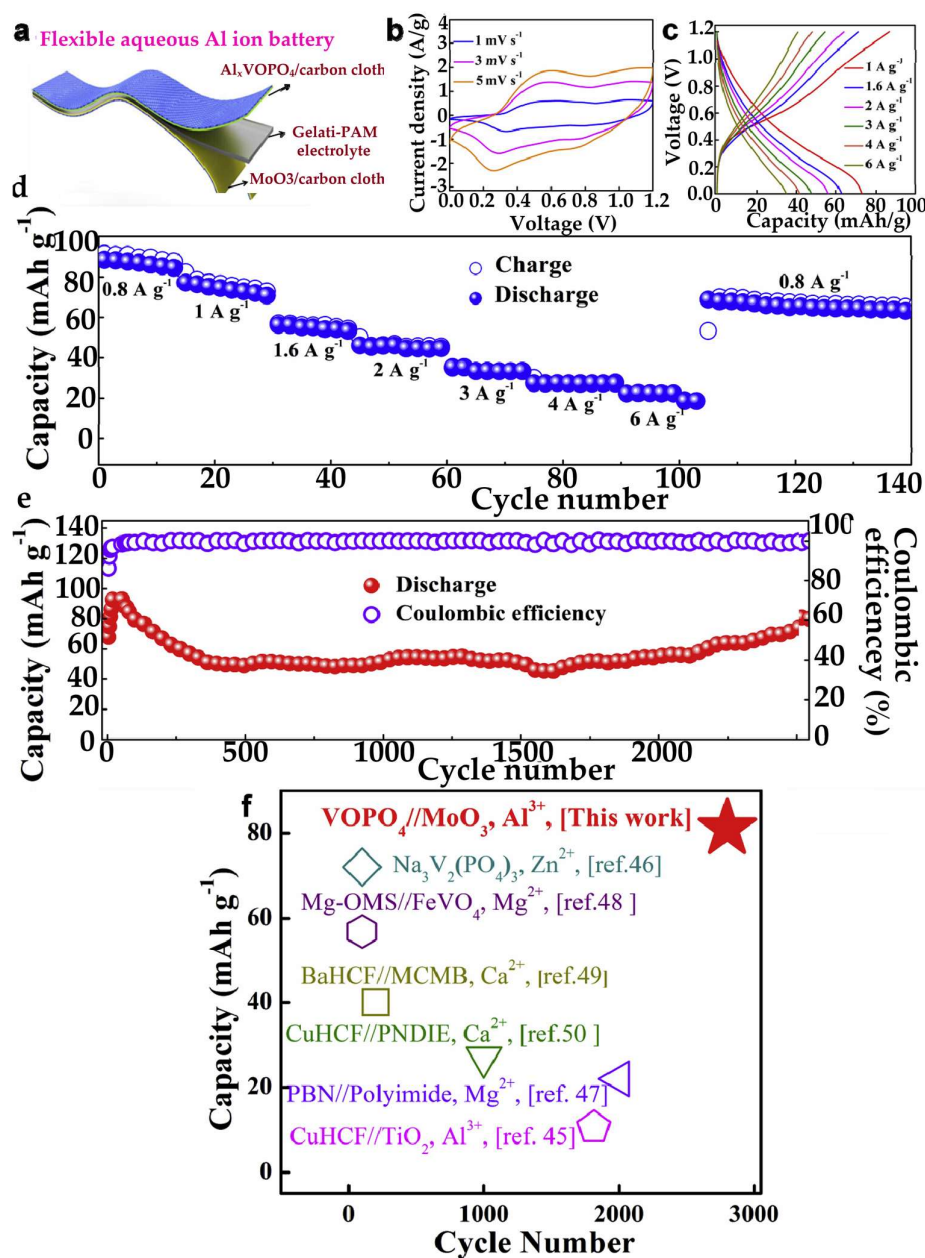


**Figure 18.** Electrochemical performance metrics of a rechargeable solid-state aqueous aluminum-ion battery (AIB). (a) Structural schematic of the flexible AIB design; (b) cyclic voltammetry profiles at varying scan rates; (c) charge–discharge curves under different current densities; (d) rate capability across multiple operating conditions; (e) long-term cycling stability and coulombic efficiency at 1 A g<sup>-1</sup>; and (f) comparative performance analysis of the presented AIB with other aqueous multivalent metal-ion battery systems, adapted with permission [191], Elsevier.

The battery used MoO<sub>3</sub> and VOPO<sub>4</sub> as intercalation electrodes. This design achieved a high rate capability (6 A g<sup>-1</sup>), discharge capacity of 88 mAh g<sup>-1</sup>, and long-term stability with 86.2% capacity retention after 2800 cycles. Notably, the battery demonstrated practical Al storage capabilities by powering electroluminescent panels of 1 m and 100 cm<sup>2</sup>, highlighting its potential for real-world applications.

To suppress alumina passivation on the aluminum anode, Xiong et al. [193] developed a PVA-based hydrogel electrolyte (PVA/Al(CF<sub>3</sub>SO<sub>3</sub>)<sub>3</sub>) (Figure 19).

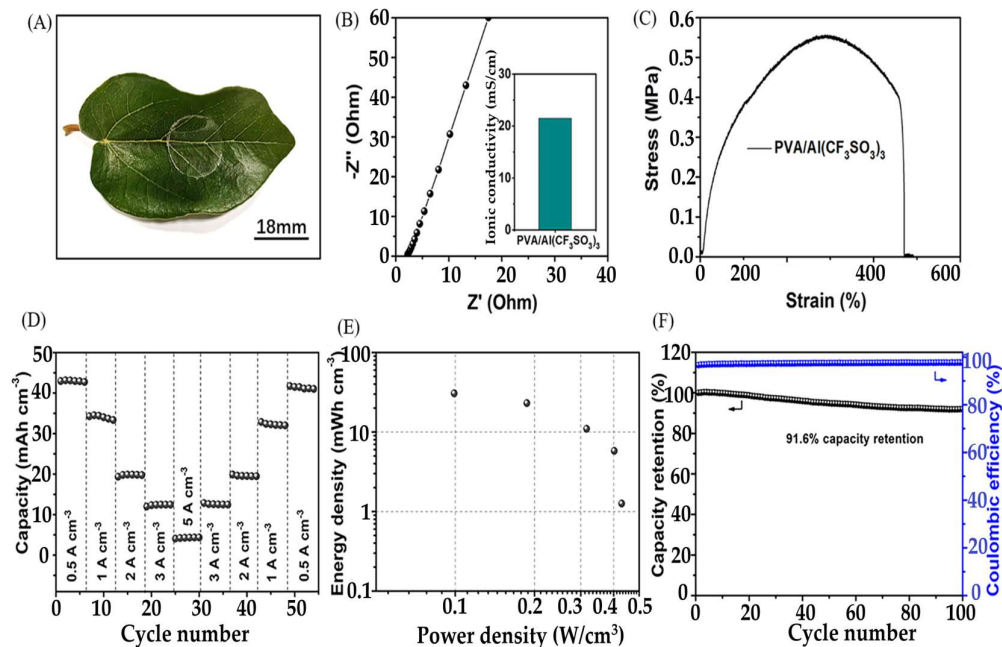


**Figure 19.** Electrochemical and mechanical characterization of PVA/Al(CF<sub>3</sub>SO<sub>3</sub>)<sub>3</sub> hydrogel electrolyte for aluminum-ion batteries. (A) Optical image of the hydrogel material; (B) AC impedance spectrum with inset showing ionic conductivity; (C) stress–strain behavior indicating mechanical robustness; (D, E) rate capability and cycling stability of the battery system; (F) long-term cycling performance of Al-ion cells using MnHCF cathode and GO/MoO<sub>3</sub> anode with hydrogel electrolyte [193].

PVA was selected for its excellent mechanical properties, high water absorbency, low cost, and non-toxic thermoplastic nature. The team fabricated a stretchable fiber-shaped AIB using a Mn-hexacyanoferrate cathode, a graphene oxide-decorated MoO<sub>3</sub> anode, and the PVA-based hydrogel. The electrolyte exhibited high ionic conductivity (21.6 mS cm<sup>-1</sup>), tensile modulus of 0.55 MPa, and strain of 461%, enabling excellent flexibility. The battery delivered a specific capacity of 42 mAh cm<sup>-3</sup> at 0.5 A cm<sup>-3</sup>, retained 91.6% capacity over 100 cycles, and achieved a specific energy of 30.6 mWh cm<sup>-3</sup>. When integrated into wearable textiles, it successfully powered an LED, demonstrating its potential for flexible and wearable electronics [193].

## 4. Challenges and Future Perspectives

### 4.1. Current Limitations in Hydrogel Applications

Hydrogels, owing to their unique properties, have garnered significant attention for a range of applications, including energy storage, sensors, and bioelectronics. However, there are several key limitations that restrict their broader integration in energy-related devices.

1. **Mechanical Strength and Durability:** Despite their impressive flexibility, many hydrogels face limitations in mechanical strength and durability, particularly when subjected to harsh operating conditions such as temperature extremes, high humidity, or mechanical deformation. This results in performance degradation, which limits their use in long-term applications like wearable electronics or energy storage systems [258].
2. **Ionic Conductivity:** The ionic conductivity of hydrogels, while suitable for some applications like supercapacitors, is often lower than that of traditional solid-state electrolytes or metal-based conductors. The challenge lies in optimizing the hydrogel matrix to improve ion transport without compromising other desirable properties such as biocompatibility and environmental.

3. **Scalability and Manufacturing:** The scalability of hydrogel-based devices, especially for large-scale energy storage applications, remains a significant hurdle. Many hydrogel-based systems are difficult to manufacture uniformly at a large scale while maintaining consistent performance.
4. **Environmental and Biodegradability Concerns:** While hydrogels are often considered eco-friendly, the degradation products of some synthetic hydrogels may raise concerns regarding their long-term environmental impact. Research is ongoing to develop fully biodegradable hydrogels that can break down harmlessly in natural environments.

#### 4.2. Potential Solutions and Advancements

In addressing these limitations, several potential solutions and advancements are being explored:

1. **Composite Hydrogels:** The incorporation of conductive materials such as carbon nanotubes, graphene, and metallic nanoparticles into hydrogel matrices has shown promise in enhancing mechanical strength and conductivity. These composite hydrogels can offer the dual benefits of improved performance and flexibility, addressing the mechanical and conductivity issues simultaneously.
2. **3D Printing and Smart Fabrication Techniques:** Advances in 3D printing and other smart fabrication methods are enabling the precise control of hydrogel structures, allowing for the creation of hydrogels with tailored properties for specific energy applications. This includes optimizing pore structures for ion transport or adjusting the polymer networks for improved mechanical integrity.
3. **Self-Healing Hydrogels:** Self-healing hydrogels, which can repair damage autonomously, offer an exciting avenue to overcome the durability challenges faced by hydrogels. By integrating dynamic covalent bonds or reversible cross-linking strategies, hydrogels can recover their function after being subjected to mechanical or environmental stress, which is crucial for ensuring long-term device reliability.
4. **Biodegradable and Sustainable Hydrogels:** Research into biodegradable and bio-based hydrogels, such as those derived from polysaccharides, is advancing rapidly. These hydrogels not only mitigate environmental concerns but also possess excellent biocompatibility, which is essential for energy devices that interact with the human body, such as wearable sensors and bioelectronics.

#### 4.3. Future Research Directions

The future of hydrogel applications in energy materials and devices is promising, but several research directions need to be pursued:

1. **Interdisciplinary Collaboration:** There is a growing need for interdisciplinary research that combines materials science, chemistry, and engineering to create hydrogels with optimized properties for specific applications. Collaborations between researchers in fields such as nanotechnology, organic electronics, and biomaterials are key to developing next-generation hydrogels for energy storage and conversion systems.
2. **High-Performance Batteries:** Further research into the optimization of hydrogels for batteries, particularly for hybrid systems that combine both, is an exciting prospect. Focus should be on improving the energy density, stability, and cycling life of these devices through innovative hydrogel formulations.

## 5. Conclusion

### 5.1. Summary of Key Points

Hydrogels represent a versatile and promising class of materials for energy storage and conversion applications. Their inherent properties—such as high water content, ionic conductivity, and mechanical adaptability—make them suitable for integration into batteries. Despite current challenges related to mechanical strength, scalability, and environmental impact, ongoing research into composite hydrogels, advanced fabrication techniques, and self-healing systems is paving the way for more robust and efficient devices. The future of hydrogel-based energy technologies lies in interdisciplinary collaboration and innovation in material design. As these materials continue to evolve, they are expected to play a critical role in shaping next-generation energy systems that are both sustainable and high-performing.

### 5.2. Impact of Hydrogels on the Future of Energy Materials and Devices

The integration of hydrogels into energy devices has the potential to revolutionize the energy sector. Hydrogels, particularly when optimized for high-performance applications, could lead to the development of more sustainable, flexible, and environmentally friendly energy storage systems. Their inherent properties, such as high-water content, ionic conductivity, and biocompatibility, make them ideal candidates for next-generation energy devices, including wearable electronics, flexible sensors, and efficient energy storage units.

### 5.3. Final Thoughts

As the field of hydrogel-based energy materials continues to evolve, the future holds great promise. Advances in material design, fabrication techniques, and functionalization strategies are expected to overcome current limitations, leading to new applications in a variety of fields, from wearable devices to large-scale energy storage systems. By addressing the challenges and pushing the boundaries of hydrogel research, these materials could play a crucial role in the development of next-generation energy systems special rechargeable batteries that are both efficient and sustainable.

**Author Contributions:** S.C.S. and N.B.: conceptualization, literature search, and writing—original draft; M.S.A.: data curation, validation; M.I.: conceptualization, writing—review and editing; and supervision; H. J.: writing—review and editing; and data curation; K. W. N.: writing—review and editing; and funding acquisition. All authors have read and agreed to the published version of the manuscript.

**Funding:** This work was supported by the National Research Foundation of Korea (NRF) grant funded by the Korean government (MSIT, grant no. 2022R1A2C2009459) and the Ministry of Trade, Industry, and Energy (MOTIE) of the Republic of Korea (No. 20224000000020).

**Data Availability Statement:** No new data were created or analyzed in this study.

**Conflicts of Interest:** The authors declare no competing interests.

## References

1. Elbinger, L.; Enke, M.; Ziegenbalg, N.; Brendel, J.C.; Schubert, U.S. Beyond Lithium-Ion Batteries: Recent Developments in Polymer-Based Electrolytes for Alternative Metal-Ion-Batteries. *Energy Storage Mater.* **2024**, *65*.
2. Sun, Y.; Shi, P.; Xiang, H.; Liang, X.; Yu, Y. High-Safety Nonaqueous Electrolytes and Interphases for Sodium-Ion Batteries. *Small* **2019**, *15*.
3. Gao, H.; Xue, L.; Xin, S.; Goodenough, J.B. A High-Energy-Density Potassium Battery with a Polymer-Gel Electrolyte and a Polyaniline Cathode. *Angew. Chemie* **2018**, *130*, doi:10.1002/ange.201802248.
4. Oh, J.S.; Ko, J.M.; Kim, D.W. Preparation and Characterization of Gel Polymer Electrolytes for Solid State Magnesium Batteries. In *Proceedings of the Electrochimica Acta*; 2004; Vol. 50.
5. Zhang, Y.; Qin, H.; Alfred, M.; Ke, H.; Cai, Y.; Wang, Q.; Huang, F.; Liu, B.; Lv, P.; Wei, Q. Reaction Modifier System Enable Double-Network Hydrogel Electrolyte for Flexible Zinc-Air Batteries with Tolerance to Extreme Cold Conditions. *Energy Storage Mater.* **2021**, *42*, doi:10.1016/j.ensm.2021.07.026.



6. Kanbua, C.; Sirichaibhinyo, T.; Rattanawongwiboon, T.; Lertsarawut, P.; Chanklinhorm, P.; Ummartyotin, S. Gamma Radiation-Induced Crosslinking of Ca<sup>2+</sup> Loaded Poly(Acrylic Acid) and Poly(Ethylene Glycol) Diacrylate Networks for Polymer Gel Electrolytes. *South African J. Chem. Eng.* **2022**, *39*, doi:10.1016/j.sajce.2021.11.007.
7. Mohammad, A.; Köhler, T.; Biswas, S.; Stöcker, H.; Meyer, D.C. A Flexible Solid-State Ionic Polymer Electrolyte for Application in Aluminum Batteries. *ACS Appl. Energy Mater.* **2023**, *6*, doi:10.1021/acsaem.2c03906.
8. Ju, Y.X.; Song, P.; Wang, P.Y.; Chen, X.X.; Chen, T.; Yao, X.H.; Zhao, W.G.; Zhang, D.Y. Cartilage Structure-Inspired Elastic Silk Nanofiber Network Hydrogel for Stretchable and High-Performance Supercapacitors. *Int. J. Biol. Macromol.* **2023**, *242*, doi:10.1016/j.ijbiomac.2023.124912.
9. Zhao, Y.; Liang, Q.; Mugo, S.M.; An, L.; Zhang, Q.; Lu, Y. Self-Healing and Shape-Editable Wearable Supercapacitors Based on Highly Stretchable Hydrogel Electrolytes. *Adv. Sci.* **2022**, *9*, doi:10.1002/advs.202201039.
10. Tadesse, M.G.; Lübben, J.F. Review on Hydrogel-Based Flexible Supercapacitors for Wearable Applications. *Gels* **2023**, *9*.
11. Ungureanu, C.; Răileanu, S.; Zgârian, R.; Tihan, G.; Burnei, C. State-of-the-Art Advances and Current Applications of Gel-Based Membranes. *Gels* **2024**, *10*.
12. Huang, J.; Wu, C.H.; Li, F.; Wang, X.; Chen, S.C. Enhancing the Proton Exchange Membrane in Tubular Air-Cathode Microbial Fuel Cells through a Hydrophobic Polymer Coating on a Hydrogel. *Materials (Basel)*. **2024**, *17*, doi:10.3390/ma17061286.
13. Bae, S.; Kim, M.; Jo, N.; Kim, K.M.; Lee, C.; Kwon, T.H.; Nam, Y.S.; Ryu, J. Amine-Rich Hydrogels for Molecular Nanoarchitectonics of Photosystem II and Inverse Opal TiO<sub>2</sub> toward Solar Water Oxidation. *ACS Appl. Mater. Interfaces* **2024**, *16*, doi:10.1021/acsaami.3c18289.
14. Armand, M.; Tarascon, J.M. Building Better Batteries. *Nature* **2008**, *451*.
15. Bruce, P.G.; Scrosati, B.; Tarascon, J.M. Nanomaterials for Rechargeable Lithium Batteries. *Angew. Chemie - Int. Ed.* **2008**, *47*.
16. Russo, R.; Becuwe, M.; Frayret, C.; Stevens, P.; Toussaint, G. Optimization of Disodium Naphthalene Dicarboxylates Negative Electrode for Organic-Inorganic Hybrid Sodium Batteries. *ECS Meet. Abstr.* **2022**, *MA2022-01*, doi:10.1149/ma2022-01194mtgabs.
17. Wang, Z.; Li, H.; Tang, Z.; Liu, Z.; Ruan, Z.; Ma, L.; Yang, Q.; Wang, D.; Zhi, C. Hydrogel Electrolytes for Flexible Aqueous Energy Storage Devices. *Adv. Funct. Mater.* **2018**, *28*.
18. Sun, Y.; Liu, N.; Cui, Y. Promises and Challenges of Nanomaterials for Lithium-Based Rechargeable Batteries. *Nat. Energy* **2016**, *1*.
19. Lee, C.; Huang, H.S.; Wang, Y.Y.; Zhang, Y.S.; Chakravarthy, R.D.; Yeh, M.Y.; Lin, H.C.; Wei, J. Stretchable, Adhesive, and Biocompatible Hydrogel Based on Iron-Dopamine Complexes. *Polymers (Basel)*. **2023**, *15*, doi:10.3390/polym15224378.
20. Chen, M.; Zhang, Y.; Xing, G.; Chou, S.L.; Tang, Y. Electrochemical Energy Storage Devices Working in Extreme Conditions. *Energy Environ. Sci.* **2021**, *14*.
21. Samantaray, S.; Mohanty, D.; Satpathy, S.K. Academic Editors: Zetian Tao and César Augusto Correia de Sequeira Molecules Exploring Recent Developments in Graphene-Based Cathode Materials for Fuel Cell Applications: A Comprehensive Overview. **2024**, doi:10.3390/molecules29122937.
22. Segura Zarate, A.Y.; Gontrani, L.; Galliano, S.; Bauer, E.M.; Donia, D.T.; Barolo, C.; Bonomo, M.; Carbone, M. Green Zinc/Galactomannan-Based Hydrogels Push up the Photovoltage of Quasi Solid Aqueous Dye Sensitized Solar Cells. *Sol. Energy* **2024**, *272*, doi:10.1016/j.solener.2024.112460.
23. Ünlü, B.; Türk, S.; Özacar, M. Novel Anti-Freeze and Self-Adhesive Gellan Gum/P3HT/LiCl Based Gel Electrolyte for Quasi Solid Dye Sensitized Solar Cells. *Colloids Surfaces A Physicochem. Eng. Asp.* **2023**, *674*, doi:10.1016/j.colsurfa.2023.131869.
24. Kanti, P.K.; K., D.J.; Swapnalini, J.; Vicki Wanasananappan, V. Advancements and Prospects of MXenes in Emerging Solar Cell Technologies. *Sol. Energy Mater. Sol. Cells* **2025**, *285*, 113540, doi:https://doi.org/10.1016/j.solmat.2025.113540.

25. Cheng, T.; Liu, Z.; Qu, J.; Meng, C.; He, L.; Li, L.; Yang, X.; Cao, Y.; Han, K.; Zhang, Y. High-Performance Organic-Inorganic Hybrid Conductive Hydrogels for Stretchable Elastic All-Hydrogel Supercapacitors and Flexible Self-Powered Integrated Systems. *Adv. Sci.* **2024**, *11*, 2403358.
26. Toyoshima, Y.; Kawamura, A.; Takashima, Y.; Miyata, T. Design of Molecularly Imprinted Hydrogels with Thermoresponsive Drug Binding Sites. *J. Mater. Chem. B* **2022**, *10*, doi:10.1039/d2tb00325b.
27. Costa, D.C.S.; Costa, P.D.C.; Gomes, M.C.; Chandrakar, A.; Wieringa, P.A.; Moroni, L.; Mano, J.F. Universal Strategy for Designing Shape Memory Hydrogels. *ACS Mater. Lett.* **2022**, *4*, doi:10.1021/acsmaterialslett.2c00107.
28. Shi, H.; Dai, Z.; Sheng, X.; Xia, D.; Shao, P.; Yang, L.; Luo, X. Conducting Polymer Hydrogels as a Sustainable Platform for Advanced Energy, Biomedical and Environmental Applications. *Sci. Total Environ.* **2021**, *786*.
29. Li, B.; Song, H.-S.; Mahamudul, M.; Rumon, H.; Mizanur, M.; Khan, R.; Jeong, J.-H. Toward Intelligent Materials with the Promise of Self-Healing Hydrogels in Flexible Devices. **2025**, doi:10.3390/polym17040542.
30. Liao, H.; Zhong, W.; Li, T.; Han, J.; Sun, X.; Tong, X.; Zhang, Y. A Review of Self-Healing Electrolyte and Their Applications in Flexible/Stretchable Energy Storage Devices. *Electrochim. Acta* **2022**, *404*.
31. Narayan, R.; Laberty-Robert, C.; Pelta, J.; Tarascon, J.M.; Dominko, R. Self-Healing: An Emerging Technology for Next-Generation Smart Batteries. *Adv. Energy Mater.* **2022**, *12*.
32. Li, H.; Zhao, H.; Song, K.; Han, F.; Liu, Z.; Tian, Q. Flexible and Stretchable Implantable Devices for Peripheral Neuromuscular Electrophysiology. *Nanoscale* **2024**, *16*.
33. Ullah, C.; Kim, A.; Lim, D.Y.; Ullah, A.; Kim, D.Y.; Lim, S.I.; Lim, H.-R. Hydrogel-Based Biointerfaces: Recent Advances, Challenges, and Future Directions in Human-Machine Integration. **2025**, doi:10.3390/gels11040232.
34. Guo, Y.; Bae, J.; Zhao, F.; Yu, G. Functional Hydrogels for Next-Generation Batteries and Supercapacitors. *Trends Chem.* **2019**, *1*.
35. Hou, R.; Gund, G.S.; Qi, K.; Nakhavivej, P.; Liu, H.; Li, F.; Xia, B.Y.; Park, H.S. Hybridization Design of Materials and Devices for Flexible Electrochemical Energy Storage. *Energy Storage Mater.* **2019**, *19*.
36. Liu, Y.; Shi, Y.; Xu, X. Evolution and Application of All-in-One Electrochemical Energy Storage System. *Energy Storage Mater.* **2021**, *41*.
37. Shi, Y.; Feng, A.; Mao, S.; Onggowarsito, C.; Stella Zhang, X.; Guo, W.; Fu, Q. Hydrogels in Solar-Driven Water and Energy Production: Recent Advances and Future Perspectives. *Chem. Eng. J.* **2024**, *492*, 152303, doi:https://doi.org/10.1016/j.cej.2024.152303.
38. Recent Advances, Y.; Duan, H.; Zhang, Y.; Zhang, Y.; Zhu, P.; Mao, Y. Citation: Duan, H Recent Advances of Stretchable Nanomaterial-Based Hydrogels for Wearable Sensors and Electrophysiological Signals Monitoring. **2024**, doi:10.3390/nano14171398.
39. Liu, D.; Huyan, C.; Wang, Z.; Guo, Z.; Zhang, X.; Torun, H.; Mulvihill, D.; Xu, B. Bin; Chen, F. Conductive Polymer Based Hydrogels and Their Application in Wearable Sensors: A Review. *Mater. Horizons* **2023**, *10*.
40. Shin, Y.; Lee, H.S.; Jeong, H.; Kim, D.-H. Recent Advances in Conductive Hydrogels for Soft Biointegrated Electronics: Materials, Properties, and Device Applications. *Wearable Electron.* **2024**, *1*, 255–280, doi:10.1016/J.WEES.2024.10.004.
41. Gashti, M.P.; Maria, J.; Moreno, C.; Chelu, M.; Popa, M. Academic Editors: Massimo Mariello Eco-Friendly Conductive Hydrogels: Towards Green Wearable Electronics. **2025**, doi:10.3390/gels11040220.
42. Sharma, A.K.; Sharma, R.; Pani, B.; Sarkar, A.; Tripathi, M. Engineering the Future with Hydrogels: Advancements in Energy Storage Devices and Biomedical Technologies †. *New J. Chem* **2024**, *48*, 10347, doi:10.1039/d4nj00881b.
43. Singh, A.N.; Meena, A.; Nam, K.W. Gels in Motion: Recent Advancements in Energy Applications. *Gels* **2024**, *10*.
44. Priya, A.S.; Kannan, K.; Henry, J.; Aepuru, R.; Shanmugaraj, K.; Pabba, D.P.; Sathish, M. Advancements in Hydrogel Materials for Next-Generation Energy Devices: Properties, Applications, and Future Prospects. *Cellulose* **2025**, doi:10.1007/s10570-025-06628-2.
45. 14 Ref 4.

46. Chen, J.; Liu, F.; Abdiryim, T.; Liu, X. An Overview of Conductive Composite Hydrogels for Flexible Electronic Devices. *Adv. Compos. Hybrid Mater.* **2024**, *7*, 35, doi:10.1007/s42114-024-00841-6.
47. Sayed, M.M. El Production of Polymer Hydrogel Composites and Their Applications. **2023**, *31*, 2855–2879, doi:10.1007/s10924-023-02796-z.
48. Lin, J.; Zheng, S.Y.; Xiao, R.; Yin, J.; Wu, Z.L.; Zheng, Q.; Qian, J. Constitutive Behaviors of Tough Physical Hydrogels with Dynamic Metal-Coordinated Bonds. *J. Mech. Phys. Solids* **2020**, *139*, doi:10.1016/j.jmps.2020.103935.
49. Tan, H.; Chu, C.R.; Payne, K.A.; Marra, K.G. Injectable in Situ Forming Biodegradable Chitosan-Hyaluronic Acid Based Hydrogels for Cartilage Tissue Engineering. *Biomaterials* **2009**, *30*, doi:10.1016/j.biomaterials.2008.12.080.
50. Priya, A.S.; Premanand, R.; Ragupathi, I.; Rao Bhaviripudi, V.; Aepuru, R.; Kannan, K.; Shanmugaraj, K. Comprehensive Review of Hydrogel Synthesis, Characterization, and Emerging Applications. **2024**, doi:10.3390/jcs8110457.
51. More, A.P.; Chapekar, S. Irradiation Assisted Synthesis of Hydrogel: A Review. *Polym. Bull.* **2024**, *81*, 5839–5908, doi:10.1007/s00289-023-05020-z.
52. Ahmed, M.S.; Islam, M.; Hasan, M.K.; Nam, K.-W. A Comprehensive Review of Radiation-Induced Hydrogels: Synthesis, Properties, and Multidimensional Applications. *Gels* **2024**, *10*, 381.
53. Raza, M.A.; Jeong, J.O.; Park, S.H. State-of-the-Art Irradiation Technology for Polymeric Hydrogel Fabrication and Application in Drug Release System. *Front. Mater.* **2021**, *8*.
54. Rickett, T.A.; Amoozgar, Z.; Tucheck, C.A.; Park, J.; Yeo, Y.; Shi, R. Rapidly Photo-Cross-Linkable Chitosan Hydrogel for Peripheral Neurosurgeries. *Biomacromolecules* **2011**, *12*, doi:10.1021/bm101004r.
55. Ishihara, M.; Obara, K.; Nakamura, S.; Fujita, M.; Masuoka, K.; Kanatani, Y.; Takase, B.; Hattori, H.; Morimoto, Y.; Ishihara, M.; et al. Chitosan Hydrogel as a Drug Delivery Carrier to Control Angiogenesis. *J. Artif. Organs* **2006**, *9*.
56. Aigoïn, J.; Payré, B.; Moncla, J.M.; Escudero, M.; Goudouneche, D.; Ferri-Angulo, D.; Calmon, P.-F.O.; Vaysse, L.; Kemoun, P.; Malaquin, L.; et al. Comparative Analysis of Electron Microscopy Techniques for Hydrogel Microarchitecture Characterization: SEM, Cryo-SEM, ESEM, and TEM. **2025**, *10*, 14687–14698, doi:10.1021/acsomega.4c08096.
57. Open Access., doi:10.1186/s13065-024-01246-8.
58. Lambrecht, S.; Biermann, M.; Kara, S.; Stefan Jopp, cd; Meyer, J. A Novel Characterization Technique for Hydrogels-in Situ Rheology-Raman Spectroscopy for Gelation and Polymerization Tracking †. *Cite this Mater. Adv* **2024**, *5*, 6957, doi:10.1039/d4ma00543k.
59. Peppas, N.A.; Keys, K.B.; Torres-Lugo, M.; Lowman, A.M. Poly(Ethylene Glycol)-Containing Hydrogels in Drug Delivery. *J. Control. Release* **1999**, *62*, doi:10.1016/S0168-3659(99)00027-9.
60. Zhang, Z.; Long, M.; Zheng, N.; Deng, Y.; Wang, Q.; Osire, T.; Xia, X. Microstructural, Physicochemical Properties, and Interaction Mechanism of Hydrogel Nanoparticles Modified by High Catalytic Activity Transglutaminase Crosslinking. *Food Hydrocoll.* **2024**, *147*, doi:10.1016/j.foodhyd.2023.109384.
61. Cortés-Camargo, S.; Román-Guerrero, A.; Alvarez-Ramirez, J.; Alpizar-Reyes, E.; Velázquez-Gutiérrez, S.K.; Pérez-Alonso, C. Microstructural Influence on Physical Properties and Release Profiles of Sesame Oil Encapsulated into Sodium Alginate-Tamarind Mucilage Hydrogel Beads. *Carbohydr. Polym. Technol. Appl.* **2023**, *5*, doi:10.1016/j.carpta.2023.100302.
62. Sharma, R.; Lallhall, A.; Puri, S.; Wangoo, N. Design of Fmoc-Phenylalanine Nanofibrillar Hydrogel and Mechanistic Studies of Its Antimicrobial Action against Both Gram-Positive and Gram-Negative Bacteria. *ACS Appl. Bio Mater.* **2023**, *6*, doi:10.1021/acsbm.2c00767.
63. Huang, H.; Yao, J.; Li, L.; Zhu, F.; Liu, Z.; Zeng, X.; Yu, X.; Huang, Z. Reinforced Polyaniline/Polyvinyl Alcohol Conducting Hydrogel from a Freezing–Thawing Method as Self-Supported Electrode for Supercapacitors. *J. Mater. Sci.* **2016**, *51*, doi:10.1007/s10853-016-0137-8.
64. Huang, H.; Chen, R.; Yang, S.; Li, L.; Liu, Y.; Huang, J. Facile Fabrication of MnO<sub>2</sub>-Embedded 3-D Porous Polyaniline Composite Hydrogel for Supercapacitor Electrode with High Loading. *High Perform. Polym.* **2020**, *32*, doi:10.1177/0954008319860893.

65. Lali Raveendran, R.; Valsala, M.; Sreenivasan Anirudhan, T. Development of Nanosilver Embedded Injectable Liquid Crystalline Hydrogel from Alginate and Chitosan for Potent Antibacterial and Anticancer Applications. *J. Ind. Eng. Chem.* **2023**, *119*, doi:10.1016/j.jiec.2022.11.044.
66. Hou, Y.; Chang, Y.; Zhao, Z.; Zhang, M.; Zhao, Q.; Guo, M.; Zhao, J.; Wu, S.; Ma, Y. Advanced In-Situ Functionalized Conductive Hydrogels with High Mechanical Strength for Hypersensitive Soft Strain Sensing Applications. *Chem. Eng. J.* **2024**, *497*, 154731, doi:https://doi.org/10.1016/j.cej.2024.154731.
67. Bouhadir, K.H.; Alsberg, E.; Mooney, D.J. Hydrogels for Combination Delivery of Antineoplastic Agents. *Biomaterials* **2001**, *22*, doi:10.1016/S0142-9612(01)00003-5.
68. Medha; Sethi, S.; Mahajan, P.; Thakur, S.; Sharma, N.; Singh, N.; Kumar, A.; Kaur, A.; Kaith, B.S. Design and Evaluation of Fluorescent Chitosan-Starch Hydrogel for Drug Delivery and Sensing Applications. *Int. J. Biol. Macromol.* **2024**, *274*, 133486, doi:https://doi.org/10.1016/j.ijbiomac.2024.133486.
69. Enoch, K.; C.S, R.; Somasundaram, A.A. Tuning the Rheological Properties of Chitosan/Alginate Hydrogels for Tissue Engineering Application. *Colloids Surfaces A Physicochem. Eng. Asp.* **2024**, *697*, 134434, doi:https://doi.org/10.1016/j.colsurfa.2024.134434.
70. Nam, S.; Hu, K.H.; Butte, M.J.; Chaudhuri, O. Strain-Enhanced Stress Relaxation Impacts Nonlinear Elasticity in Collagen Gels. *Proc. Natl. Acad. Sci. U. S. A.* **2016**, *113*, doi:10.1073/pnas.1523906113.
71. Zhang, W.; Liu, S.; Wang, L.; Li, B.; Xie, M.; Deng, Y.; Zhang, J.; Zeng, H.; Qiu, L.; Huang, L.; et al. Triple-Crosslinked Double-Network Alginate/Dextran/Dendrimer Hydrogel with Tunable Mechanical and Adhesive Properties: A Potential Candidate for Sutureless Keratoplasty. *Carbohydr. Polym.* **2024**, *344*, 122538, doi:https://doi.org/10.1016/j.carbpol.2024.122538.
72. Cacopardo, L.; Guazzelli, N.; Nossa, R.; Mattei, G.; Ahluwalia, A. Engineering Hydrogel Viscoelasticity. *J. Mech. Behav. Biomed. Mater.* **2019**, *89*, doi:10.1016/j.jmbbm.2018.09.031.
73. Ling, W.; Wang, P.; Chen, Z.; Wang, H.; Wang, J.; Ji, Z.; Fei, J.; Ma, Z.; He, N.; Huang, Y. Nanostructure Design Strategies for Aqueous Zinc-Ion Batteries. *ChemElectroChem* **2020**, *7*.
74. Yang, P.; Yang, J.L.; Liu, K.; Fan, H.J. Hydrogels Enable Future Smart Batteries. *ACS Nano*. **2022**, *16*, 15528.
75. Liu, W.; Li, L.; Yue, S.; Jia, S.; Wang, C.; Zhang, D. Electrolytes for Aluminum-Ion Batteries: Progress and Outlook. *Chem. Eur. J.* **2024**, *30*, e202402017.
76. Liu, Y.K.; Zhao, C.Z.; Du, J.; Zhang, X.Q.; Chen, A.B.; Zhang, Q. Research Progresses of Liquid Electrolytes in Lithium-Ion Batteries. *Small* **2023**, *19*.
77. Zhang, Y.; Yuan, Z.; Zhao, L.; Li, Y.; Qin, X.; Li, J.; Han, W.; Wang, L. Review of Design Routines of MXene Materials for Magnesium-Ion Energy Storage Device. *Small* **2023**, *19*.
78. Gill, S.; Dhankhar, M. Sodium Ion (Na<sup>+</sup>) Batteries—a Comprehensive Review. *Mater. Nanosci.* **2024**, *11*, 951.
79. Janek, J.; Zeier, W.G. A Solid Future for Battery Development. *Nat. Energy* **2016**, *1*.
80. Muldoon, J.; Bucur, C.B.; Gregory, T. Quest for Nonaqueous Multivalent Secondary Batteries: Magnesium and Beyond. *Chem. Rev.* **2014**, *114*.
81. Islam, M.; Ahmed, M.S.; Han, D.; Bari, G.A.K.M.R.; Nam, K.-W. Electrochemical Storage Behavior of a High-Capacity Mg-Doped P2-Type Na<sub>2</sub>/3Fe<sub>1-y</sub>MnyO<sub>2</sub> Cathode Material Synthesized by a Sol-Gel Method. *Gels* **2024**, *10*, 24.
82. Hwang, S.; Kim, D.H.; Shin, J.H.; Jang, J.E.; Ahn, K.H.; Lee, C.; Lee, H. Ionic Conduction and Solution Structure in LiPF<sub>6</sub> and LiBF<sub>4</sub> Propylene Carbonate Electrolytes. *J. Phys. Chem. C* **2018**, *122*, doi:10.1021/acs.jpcc.8b06035.
83. Bae, J.; Qian, Y.; Li, Y.; Zhou, X.; Goodenough, J.B.; Yu, G. Polar Polymer-Solvent Interaction Derived Favorable Interphase for Stable Lithium Metal Batteries. *Energy Environ. Sci.* **2019**, *12*, doi:10.1039/c9ee02558h.
84. Yang, C.; Chen, J.; Qing, T.; Fan, X.; Sun, W.; von Cresce, A.; Ding, M.S.; Borodin, O.; Vatamanu, J.; Schroeder, M.A.; et al. 4.0 V Aqueous Li-Ion Batteries. *Joule* **2017**, *1*, doi:10.1016/j.joule.2017.08.009.
85. Feig, V.R.; Tran, H.; Lee, M.; Bao, Z. Mechanically Tunable Conductive Interpenetrating Network Hydrogels That Mimic the Elastic Moduli of Biological Tissue. *Nat. Commun.* **2018**, *9*, doi:10.1038/s41467-018-05222-4.
86. Islam, M.; Ahmed, M.S.; Faizan, M.; Ali, B.; Bhuyan, M.M.; Bari, G.A.K.M.R.; Nam, K.-W. Review on the Polymeric and Chelate Gel Precursor for Li-Ion Battery Cathode Material Synthesis. *Gels* **2024**, *10*, 586.



87. Ohzuku, T.; Ueda, A. Solid-State Redox Reactions of LiCoO<sub>2</sub> (R3m) for 4 Volt Secondary Lithium Cells. *J. Electrochem. Soc.* **1994**, *141*, doi:10.1149/1.2059267.
88. Tang, Y.; Zhang, Y.; Rui, X.; Qi, D.; Luo, Y.; Leow, W.R.; Chen, S.; Guo, J.; Wei, J.; Li, W.; et al. Conductive Inks Based on a Lithium Titanate Nanotube Gel for High-Rate Lithium-Ion Batteries with Customized Configuration. *Adv. Mater.* **2016**, *28*, doi:10.1002/adma.201505161.
89. Zhang, J.; Shi, Y.; Ding, Y.; Zhang, W.; Yu, G. In Situ Reactive Synthesis of Polypyrrole-MnO<sub>2</sub> Coaxial Nanotubes as Sulfur Hosts for High-Performance Lithium-Sulfur Battery. *Nano Lett.* **2016**, *16*, doi:10.1021/acs.nanolett.6b03849.
90. Wu, H.; Wang, X.; Jiang, L.; Wu, C.; Zhao, Q.; Liu, X.; Hu, B.; Yi, L. The Effects of Electrolyte on the Supercapacitive Performance of Activated Calcium Carbide-Derived Carbon. *J. Power Sources* **2013**, *226*, doi:10.1016/j.jpowsour.2012.11.014.
91. Xiao, W.; Zhou, W.; Yu, H.; Pu, Y.; Zhang, Y.; Hu, C. Template Synthesis of Hierarchical Mesoporous δ-MnO<sub>2</sub> Hollow Microspheres as Electrode Material for High-Performance Symmetric Supercapacitor. *Electrochim. Acta* **2018**, *264*, doi:10.1016/j.electacta.2018.01.070.
92. Ojeda, M.; Chen, B.; Leung, D.Y.C.; Xuan, J.; Wang, H. A Hydrogel Template Synthesis of TiO<sub>2</sub> Nanoparticles for Aluminium-Ion Batteries. In Proceedings of the Energy Procedia; 2017; Vol. 105.
93. Kwon, K.A.; Lim, H.S.; Sun, Y.K.; Suh, K. Do α-Fe<sub>2</sub>O<sub>3</sub> Submicron Spheres with Hollow and Macroporous Structures as High-Performance Anode Materials for Lithium Ion Batteries. *J. Phys. Chem. C* **2014**, *118*, doi:10.1021/jp5000057.
94. Hasegawa, G.; Ishihara, Y.; Kanamori, K.; Miyazaki, K.; Yamada, Y.; Nakanishi, K.; Abe, T. Facile Preparation of Monolithic LiFePO<sub>4</sub>/Carbon Composites with Well-Defined Macropores for a Lithium-Ion Battery. *Chem. Mater.* **2011**, *23*, doi:10.1021/cm2021438.
95. Zhang, J.; Huang, H.; Bae, J.; Chung, S.H.; Zhang, W.; Manthiram, A.; Yu, G. Nanostructured Host Materials for Trapping Sulfur in Rechargeable Li-S Batteries: Structure Design and Interfacial Chemistry. *Small Methods* **2018**, *2*.
96. Yang, Y.; Yu, G.; Cha, J.J.; Wu, H.; Vosgueritchian, M.; Yao, Y.; Bao, Z.; Cui, Y. Improving the Performance of Lithium-Sulfur Batteries by Conductive Polymer Coating. *ACS Nano* **2011**, *5*, doi:10.1021/nn203436j.
97. Kim, W.J.; Kang, J.G.; Kim, D.W. Fibrin Biopolymer Hydrogel-Templated 3D Interconnected Si@C Framework for Lithium Ion Battery Anodes. *Appl. Surf. Sci.* **2021**, *551*, doi:10.1016/j.apsusc.2021.149439.
98. Introduction and Adhesion Theories. In *Adhesives Technology Handbook*; 2009.
99. Li, G.; Li, C.; Li, G.; Yu, D.; Song, Z.; Wang, H.; Liu, X.; Liu, H.; Liu, W. Development of Conductive Hydrogels for Fabricating Flexible Strain Sensors. *Small* **2022**, *18*.
100. Herrmann, A.; Haag, R.; Schedler, U. Hydrogels and Their Role in Biosensing Applications. *Adv. Healthc. Mater.* **2021**, *10*.
101. Zou, F.; Manthiram, A. A Review of the Design of Advanced Binders for High-Performance Batteries. *Adv. Energy Mater.* **2020**, *10*.
102. Chen, C.; Lee, S.H.; Cho, M.; Kim, J.; Lee, Y. Cross-Linked Chitosan as an Efficient Binder for Si Anode of Li-Ion Batteries. *ACS Appl. Mater. Interfaces* **2016**, *8*, doi:10.1021/acsami.5b10673.
103. Liu, X.; Yao, R.; Wang, S.; Wei, Y.; Chen, B.; Liang, W.; Tian, C.; Nie, C.; Li, D.; Chen, Y. Rational Design of Stretchable and Conductive Hydrogel Binder for Highly Reversible SiP<sub>2</sub> Anode. *J. Energy Chem.* **2023**, *83*, doi:10.1016/j.jechem.2023.04.037.
104. Yang, B.; Liu, F.; Liu, Y.; Dong, J.; Liu, M.; Wang, S.; Zhang, L. Self-Assembled Three-Dimensional Si/Carbon Frameworks as Promising Lithium-Ion Battery Anode. *J. Power Sources* **2023**, *553*, doi:10.1016/j.jpowsour.2022.232274.
105. Weng, Z.; Di, S.; Chen, L.; Wu, G.; Zhang, Y.; Jia, C.; Zhang, N.; Liu, X.; Chen, G. Random Copolymer Hydrogel as Elastic Binder for the SiO<sub>x</sub> Microparticle Anode in Lithium-Ion Batteries. *ACS Appl. Mater. Interfaces* **2022**, *14*, doi:10.1021/acsami.2c12128.
106. Mu, P.; Sun, C.; Gao, C.; Li, L.; Zhang, H.; Li, J.; Li, C.; Dong, S.; Cui, G. Dual Network Electrode Binder toward Practical Lithium-Sulfur Battery Applications. *ACS Energy Lett.* **2023**, *8*, doi:10.1021/acsenergylett.3c01038.

107. Chen, Z.; To, J.W.F.; Wang, C.; Lu, Z.; Liu, N.; Chortos, A.; Pan, L.; Wei, F.; Cui, Y.; Bao, Z. A Three-Dimensionally Interconnected Carbon Nanotube-Conducting Polymer Hydrogel Network for High-Performance Flexible Battery Electrodes. *Adv. Energy Mater.* **2014**, *4*, doi:10.1002/aenm.201400207.
108. Wu, H.; Yan, C.; Xu, L.; Xu, N.; Wu, X.; Jiang, Z.; Zhu, S.; Diao, G.; Chen, M. Super Flexible Cathode Material with 3D Cross-Linking System Based on Polyvinyl Alcohol Hydrogel for Boosting Aqueous Zinc Ion Batteries. *ChemElectroChem* **2022**, *9*, doi:10.1002/celec.202200288.
109. Wang, W.; Ding, J.; Liu, Z.; Wei, Y.; Cheng, W.; Liu, Q.; Zhang, W.; Wang, X.C.; Zhang, W.; Wang, B.; et al. Novel-Designed Cobweb-like Binder by “Four-in-One” Strategy for High Performance SiO Anode. *Chem. Eng. J.* **2023**, *458*, doi:10.1016/j.cej.2023.141387.
110. Liu, J.; Zhang, Q.; Wu, Z.Y.; Wu, J.H.; Li, J.T.; Huang, L.; Sun, S.G. A High-Performance Alginate Hydrogel Binder for the Si/C Anode of a Li-Ion Battery. *Chem. Commun.* **2014**, *50*, doi:10.1039/c4cc00081a.
111. Wang, J.; Ye, T.; Li, Y.; Wang, L.; Li, L.; Li, F.; He, E.; Zhang, Y. Ultrasoft All-Hydrogel Aqueous Lithium-Ion Battery with a Coaxial Fiber Structure. *Polym. J.* **2022**, *54*, doi:10.1038/s41428-022-00688-y.
112. Zhao, M.; Li, B.Q.; Zhang, X.Q.; Huang, J.Q.; Zhang, Q. A Perspective toward Practical Lithium-Sulfur Batteries. *ACS Cent. Sci.* **2020**, *6*, doi:10.1021/acscentsci.0c00449.
113. Liu, B.; Bo, R.; Taheri, M.; Di Bernardo, I.; Motta, N.; Chen, H.; Tsuzuki, T.; Yu, G.; Tricoli, A. Metal-Organic Frameworks/Conducting Polymer Hydrogel Integrated Three-Dimensional Free-Standing Monoliths as Ultrahigh Loading Li-S Battery Electrodes. *Nano Lett.* **2019**, *19*, doi:10.1021/acs.nanolett.9b01033.
114. Xu, G.L.; Gong, Y.D.; Miao, C.; Wang, Q.; Nie, S.Q.; Xin, Y.; Wen, M.Y.; Liu, J.; Xiao, W. Sn Nanoparticles Embedded into Porous Hydrogel-Derived Pyrolytic Carbon as Composite Anode Materials for Lithium-Ion Batteries. *Rare Met.* **2022**, *41*, doi:10.1007/s12598-022-02073-3.
115. Xu, T.; Liu, K.; Sheng, N.; Zhang, M.; Liu, W.; Liu, H.; Dai, L.; Zhang, X.; Si, C.; Du, H.; et al. Biopolymer-Based Hydrogel Electrolytes for Advanced Energy Storage/Conversion Devices: Properties, Applications, and Perspectives. *Energy Storage Mater.* **2022**, *48*.
116. Ahmed, M.S.; Islam, M.; Raut, B.; Yun, S.; Kim, H.Y.; Nam, K.-W. A Comprehensive Review of Functional Gel Polymer Electrolytes and Applications in Lithium-Ion Battery. *Gels* **2024**, *10*, 563. <https://doi.org/10.3390/gels10090563>
117. Lu, C.; Chen, X. All-Temperature Flexible Supercapacitors Enabled by Antifreezing and Thermally Stable Hydrogel Electrolyte. *Nano Lett.* **2020**, *20*, doi:10.1021/acs.nanolett.9b05148.
118. Ma, L.; Chen, S.; Wang, D.; Yang, Q.; Mo, F.; Liang, G.; Li, N.; Zhang, H.; Zapfen, J.A.; Zhi, C. Super-Stretchable Zinc–Air Batteries Based on an Alkaline-Tolerant Dual-Network Hydrogel Electrolyte. *Adv. Energy Mater.* **2019**, *9*, doi:10.1002/aenm.201803046.
119. Liu, J.; Yang, C.; Chi, X.; Wen, B.; Wang, W.; Liu, Y. Water/Sulfolane Hybrid Electrolyte Achieves Ultralow-Temperature Operation for High-Voltage Aqueous Lithium-Ion Batteries. *Adv. Funct. Mater.* **2022**, *32*, doi:10.1002/adfm.202106811.
120. Yang, Y.; Chen, Z.; Lv, T.; Dong, K.; Liu, Y.; Qi, Y.; Cao, S.; Chen, T. Ultrafast Self-Assembly of Supramolecular Hydrogels toward Novel Flame-Retardant Separator for Safe Lithium Ion Battery. *J. Colloid Interface Sci.* **2023**, *649*, doi:10.1016/j.jcis.2023.06.058.
121. Yang, Y.; Bai, Z.; Liu, S.; Zhu, Y.; Zheng, J.; Chen, G.; Huang, B. Self-Protecting Aqueous Lithium-Ion Batteries. *Small* **2022**, *18*, doi:10.1002/smll.202203035.
122. Li, X.; Zeng, S.; Li, W.; Lin, H.; Zhong, H.; Zhu, H.; Mai, Y. Stretchable Hydrogel Electrolyte Films Based on Moisture Self-Absorption for Flexible Quasi-Solid-State Batteries. *Chem. Eng. J.* **2022**, *439*, doi:10.1016/j.cej.2022.135741.
123. Bae, J.; Li, Y.; Zhang, J.; Zhou, X.; Zhao, F.; Shi, Y.; Goodenough, J.B.; Yu, G. A 3D Nanostructured Hydrogel-Framework-Derived High-Performance Composite Polymer Lithium-Ion Electrolyte. *Angew. Chemie - Int. Ed.* **2018**, *57*, doi:10.1002/anie.201710841.
124. Cao, X.; Tan, D.; Guo, Q.; Zhang, T.; Hu, F.; Sun, N.; Huang, J.; Fang, C.; Ji, R.; Bi, S.; et al. High-Performance Fully-Stretchable Solid-State Lithium-Ion Battery with a Nanowire-Network Configuration and Crosslinked Hydrogel. *J. Mater. Chem. A* **2022**, *10*, doi:10.1039/d2ta00425a.

125. Pei, Z.; Yuan, Z.; Wang, C.; Zhao, S.; Fei, J.; Wei, L.; Chen, J.; Wang, C.; Qi, R.; Liu, Z.; Chen, Y.. AFlexible RechargeableZinc–Air Battery with Excellent Low-Temperature Adaptability. *Angew.Chem. Int.Ed.* **2020**, *59*, 4793 <https://doi.org/10.1002/anie.201915836>.
126. Zhu, M.; Wang, X.; Tang, H.; Wang, J.; Hao, Q.; Liu, L.; Li, Y.; Zhang, K.; Schmidt, O.G. Antifreezing Hydrogel with High Zinc Reversibility for Flexible and Durable Aqueous Batteries by Cooperative Hydrated Cations. *Adv. Funct. Mater.* **2020**, *30*, doi:10.1002/adfm.201907218.
127. Yang, C.; Chen, J.; Ji, X.; Pollard, T.P.; Lü, X.; Sun, C.J.; Hou, S.; Liu, Q.; Liu, C.; Qing, T.; et al. Aqueous Li-Ion Battery Enabled by Halogen Conversion–Intercalation Chemistry in Graphite. *Nature* **2019**, *569*, doi:10.1038/s41586-019-1175-6.
128. Strachan, N.; Fais, B.; Daly, H. Reinventing the Energy Modelling–Policy Interface. *Nat. Energy* **2016**, *1*.
129. Le Floch, P.; Yao, X.; Liu, Q.; Wang, Z.; Nian, G.; Sun, Y.; Jia, L.; Suo, Z. Wearable and Washable Conductors for Active Textiles. *ACS Appl. Mater. Interfaces* **2017**, *9*, doi:10.1021/acsami.7b07361.
130. Yuk, H.; Zhang, T.; Parada, G.A.; Liu, X.; Zhao, X. Skin-Inspired Hydrogel-Elastomer Hybrids with Robust Interfaces and Functional Microstructures. *Nat. Commun.* **2016**, *7*, doi:10.1038/ncomms12028.
131. Sun, J.Y.; Keplinger, C.; Whitesides, G.M.; Suo, Z. Ionic Skin. *Adv. Mater.* **2014**, *26*, doi:10.1002/adma.201403441.
132. Suo, L.; Borodin, O.; Gao, T.; Olguin, M.; Ho, J.; Fan, X.; Luo, C.; Wang, C.; Xu, K. “Water-in-Salt” Electrolyte Enables High-Voltage Aqueous Lithium-Ion Chemistries. *Science (80-. )*. **2015**, *350*, doi:10.1126/science.aab1595.
133. Zhou, W.; Zheng, Y.; Zartashia, M.; Shan, Y.; Noor, H.; Lou, H.; Hou, X. Aqueous Dual-Electrolyte Full-Cell System for Improving Energy Density of Sodium-Ion Batteries. *ACS Appl. Mater. Interfaces* **2022**, *14*, doi:10.1021/acsami.2c06304.
134. Yang, M.; Luo, J.; Guo, X.; Chen, J.; Cao, Y.; Chen, W. Aqueous Rechargeable Sodium-Ion Batteries: From Liquid to Hydrogel. *Batteries* **2022**, *8*.
135. Casas, X.; Niederberger, M.; Lizundia, E. A Sodium-Ion Battery Separator with Reversible Voltage Response Based on Water-Soluble Cellulose Derivatives. *ACS Appl. Mater. Interfaces* **2020**, *12*, doi:10.1021/acsami.0c05262.
136. Cheng, C.; Zang, X.; Hou, W.; Li, C.; Huang, Q.; Hu, X.; Sun, C.; Zhang, Y.; Yang, J.; Ma, F. Construction of Three-Dimensional Electronic Interconnected Na<sub>3</sub>V<sub>2</sub>(PO<sub>4</sub>)<sub>3</sub>/C as Cathode for Sodium Ion Batteries. *J. Alloys Compd.* **2022**, *899*, doi:10.1016/j.jallcom.2021.163363.
137. Zhong, L.; Lu, Y.; Li, H.; Tao, Z.; Chen, J. High-Performance Aqueous Sodium-Ion Batteries with Hydrogel Electrolyte and Alloxazine/CMK-3 Anode. *ACS Sustain. Chem. Eng.* **2018**, *6*, doi:10.1021/acssuschemeng.8b00663.
138. Yan, Y.; Ma, Z.; Lin, H.; Rui, K.; Zhang, Q.; Wang, Q.; Du, M.; Li, D.; Zhang, Y.; Zhu, J.; et al. Hydrogel Self-Templated Synthesis of Na<sub>3</sub>V<sub>2</sub>(PO<sub>4</sub>)<sub>3</sub>@CNT Porous Network as Ultrastable Cathode for Sodium-Ion Batteries. *Compos. Commun.* **2019**, *13*, doi:10.1016/j.coco.2019.03.006.
139. Cheng, Y.; Chi, X.; Yang, J.; Liu, Y. Cost Attractive Hydrogel Electrolyte for Low Temperature Aqueous Sodium Ion Batteries. *J. Energy Storage* **2021**, *40*, doi:10.1016/j.est.2021.102701.
140. Mittal, N.; Tien, S.; Lizundia, E.; Niederberger, M. Hierarchical Nanocellulose-Based Gel Polymer Electrolytes for Stable Na Electrodeposition in Sodium Ion Batteries. *Small* **2022**, *18*, doi:10.1002/sml.202107183.
141. Zhang, S.; Li, S.; Li, L.; Wen, D.; Peng, X.; Zhang, H. Urchin-like MoS<sub>2</sub>/MoO<sub>2</sub> Microspheres Coated with GO Hydrogel: Achieve a Long-Term Cyclability as Anode for Sodium Ion Batteries. *Mater. Today Sustain.* **2023**, *21*, doi:10.1016/j.mtsust.2022.100289.
142. Zhang, X.; Hu, J.P.; Fu, N.; Zhou, W. Bin; Liu, B.; Deng, Q.; Wu, X.W. Comprehensive Review on Zinc-Ion Battery Anode: Challenges and Strategies. *InfoMat* **2022**, *4*.
143. Yan, J.; Ang, E.H.; Yang, Y.; Zhang, Y.; Ye, M.; Du, W.; Li, C.C. High-Voltage Zinc-Ion Batteries: Design Strategies and Challenges. *Adv. Funct. Mater.* **2021**, *31*.
144. Zuo, Y.; Wang, K.; Pei, P.; Wei, M.; Liu, X.; Xiao, Y.; Zhang, P. Zinc Dendrite Growth and Inhibition Strategies. *Mater. Today Energy* **2021**, *20*.

145. Lv, Y.; Xiao, Y.; Ma, L.; Zhi, C.; Chen, S. Recent Advances in Electrolytes for “Beyond Aqueous” Zinc-Ion Batteries. *Adv. Mater.* **2022**, *34*.
146. Shi, Y.; Chen, Y.; Shi, L.; Wang, K.; Wang, B.; Li, L.; Ma, Y.; Li, Y.; Sun, Z.; Ali, W.; et al. An Overview and Future Perspectives of Rechargeable Zinc Batteries. *Small* **2020**, *16*.
147. Selis, L.A.; Seminario, J.M. Dendrite Formation in Li-Metal Anodes: An Atomistic Molecular Dynamics Study. *RSC Adv.* **2019**, *9*, doi:10.1039/c9ra05067a.
148. Li, B.; Chao, Y.; Li, M.; Xiao, Y.; Li, R.; Yang, K.; Cui, X.; Xu, G.; Li, L.; Yang, C.; et al. A Review of Solid Electrolyte Interphase (SEI) and Dendrite Formation in Lithium Batteries. *Electrochem. Energy Rev.* **2023**, *6*.
149. Mittal, N.; Ojanguren, A.; Kundu, D.; Lizundia, E.; Niederberger, M. Bottom-Up Design of a Green and Transient Zinc-Ion Battery with Ultralong Lifespan. *Small* **2023**, *19*, doi:10.1002/sml.202206249.
150. Yang, J.L.; Li, J.; Zhao, J.W.; Liu, K.; Yang, P.; Fan, H.J. Stable Zinc Anodes Enabled by a Zincophilic Polyanionic Hydrogel Layer. *Adv. Mater.* **2022**, *34*, doi:10.1002/adma.202202382.
151. Park, J.H.; Hyun Park, S.; Joung, D.; Kim, C. Sustainable Biopolymeric Hydrogel Interphase for Dendrite-Free Aqueous Zinc-Ion Batteries. *Chem. Eng. J.* **2022**, *433*, doi:10.1016/j.cej.2021.133532.
152. Cong, J.; Shen, X.; Wen, Z.; Wang, X.; Peng, L.; Zeng, J.; Zhao, J. Ultra-Stable and Highly Reversible Aqueous Zinc Metal Anodes with High Preferred Orientation Deposition Achieved by a Polyanionic Hydrogel Electrolyte. *Energy Storage Mater.* **2021**, *35*, doi:10.1016/j.ensm.2020.11.041.
153. Chan, C.Y.; Wang, Z.; Li, Y.; Yu, H.; Fei, B.; Xin, J.H. Single-Ion Conducting Double-Network Hydrogel Electrolytes for Long Cycling Zinc-Ion Batteries. *ACS Appl. Mater. Interfaces* **2021**, *13*, doi:10.1021/acsami.1c05941.
154. Fu, C.; Wang, Y.; Lu, C.; Zhou, S.; He, Q.; Hu, Y.; Feng, M.; Wan, Y.; Lin, J.; Zhang, Y.; et al. Modulation of Hydrogel Electrolyte Enabling Stable Zinc Metal Anode. *Energy Storage Mater.* **2022**, *51*, doi:10.1016/j.ensm.2022.06.034.
155. Ling, W.; Mo, F.; Wang, J.; Liu, Q.; Liu, Y.; Yang, Q.; Qiu, Y.; Huang, Y. Self-Healable Hydrogel Electrolyte for Dendrite-Free and Self-Healable Zinc-Based Aqueous Batteries. *Mater. Today Phys.* **2021**, *20*, doi:10.1016/j.mtphys.2021.100458.
156. Liu, Y.; He, H.; Gao, A.; Ling, J.; Yi, F.; Hao, J.; Li, Q.; Shu, D. Fundamental Study on Zn Corrosion and Dendrite Growth in Gel Electrolyte towards Advanced Wearable Zn-Ion Battery. *Chem. Eng. J.* **2022**, *446*, doi:10.1016/j.cej.2022.137021.
157. Ji, S.; Qin, J.; Yang, S.; Shen, P.; Hu, Y.; Yang, K.; Luo, H.; Xu, J. A Mechanically Durable Hybrid Hydrogel Electrolyte Developed by Controllable Accelerated Polymerization Mechanism towards Reliable Aqueous Zinc-Ion Battery. *Energy Storage Mater.* **2023**, *55*, doi:10.1016/j.ensm.2022.11.050.
158. Zhu, R.; Yang, H.; Cui, W.; Fadillah, L.; Huang, T.; Xiong, Z.; Tang, C.; Kowalski, D.; Kitano, S.; Zhu, C.; et al. High Strength Hydrogels Enable Dendrite-Free Zn Metal Anodes and High-Capacity Zn-MnO<sub>2</sub> Batteries via a Modified Mechanical Suppression Effect. *J. Mater. Chem. A* **2022**, *10*, doi:10.1039/d1ta10079c.
159. Li, L.; Zhang, L.; Guo, W.; Chang, C.; Wang, J.; Cong, Z.; Pu, X. High-Performance Dual-Ion Zn Batteries Enabled by a Polyzwitterionic Hydrogel Electrolyte with Regulated Anion/Cation Transport and Suppressed Zn Dendrite Growth. *J. Mater. Chem. A* **2021**, *9*, doi:10.1039/d1ta08127f.
160. Dong, H.; Li, J.; Zhao, S.; Jiao, Y.; Chen, J.; Tan, Y.; Brett, D.J.L.; He, G.; Parkin, I.P. Investigation of a Biomass Hydrogel Electrolyte Naturally Stabilizing Cathodes for Zinc-Ion Batteries. *ACS Appl. Mater. Interfaces* **2021**, *13*, doi:10.1021/acsami.0c20388.
161. Xu, L.; Meng, T.; Zheng, X.; Li, T.; Brozena, A.H.; Mao, Y.; Zhang, Q.; Clifford, B.C.; Rao, J.; Hu, L. Nanocellulose-Carboxymethylcellulose Electrolyte for Stable, High-Rate Zinc-Ion Batteries. *Adv. Funct. Mater.* **2023**, *33*, doi:10.1002/adfm.202302098.
162. Wang, Y.; Li, Q.; Hong, H.; Yang, S.; Zhang, R.; Wang, X.; Jin, X.; Xiong, B.; Bai, S.; Zhi, C. Lean-Water Hydrogel Electrolyte for Zinc Ion Batteries. *Nat. Commun.* **2023**, *14*, doi:10.1038/s41467-023-39634-8.
163. Ma, D.; Yuan, D.; Ponce de León, C.; Jiang, Z.; Xia, X.; Pan, J. Current Progress and Future Perspectives of Electrolytes for Rechargeable Aluminum-Ion Batteries. *Energy Environ. Mater.* **2023**, *6*.
164. Lv, R.; Wu, H.; Jiang, Z.; Zheng, A.; Yu, H.; Chen, M. Flexible Hydrogel Compound of V<sub>2</sub>O<sub>5</sub>/GO/PVA for Enhancing Mechanical and Zinc Storage Performances. *Electrochim. Acta* **2022**, *429*, doi:10.1016/j.electacta.2022.140998.



165. Li, Z.; Zhou, G.; Ye, L.; He, J.; Xu, W.; Hong, S.; Chen, W.; Li, M.C.; Liu, C.; Mei, C. High-Energy and Dendrite-Free Solid-State Zinc Metal Battery Enabled by a Dual-Network and Water-Confinement Hydrogel Electrolyte. *Chem. Eng. J.* **2023**, *472*, doi:10.1016/j.cej.2023.144992.
166. Zhang, H.; Wang, R.; Hu, Y.; Wang, R.; Shen, J.; Mao, Y.; Wu, Q.; Wang, B. Achieving Highly Reversible Zn Anodes by Inhibiting the Activity of Free Water Molecules and Manipulating Zn Deposition in a Hydrogel Electrolyte. *ACS Appl. Energy Mater.* **2023**, *6*, doi:10.1021/acsaem.3c00831.
167. Lu, H.; Hu, J.; Wei, X.; Zhang, K.; Xiao, X.; Zhao, J.; Hu, Q.; Yu, J.; Zhou, G.; Xu, B. A Recyclable Biomass Electrolyte towards Green Zinc-Ion Batteries. *Nat. Commun.* **2023**, *14*, doi:10.1038/s41467-023-40178-0.
168. Zhang, H.; Liu, X.; Li, H.; Qin, B.; Passerini, S. High-Voltage Operation of a V2O5 Cathode in a Concentrated Gel Polymer Electrolyte for High-Energy Aqueous Zinc Batteries. *ACS Appl. Mater. Interfaces* **2020**, *12*, doi:10.1021/acsaami.0c02102.
169. Sun, L.; Yao, Y.; Dai, L.; Jiao, M.; Ding, B.; Yu, Q.; Tang, J.; Liu, B. Sustainable and High-Performance Zn Dual-Ion Batteries with a Hydrogel-Based Water-in-Salt Electrolyte. *Energy Storage Mater.* **2022**, *47*, doi:10.1016/j.ensm.2022.02.012.
170. Li, C.; Zhang, K.; Cheng, X.; Li, J.; Jiang, Y.; Li, P.; Wang, B.; Peng, H. Polymers for Flexible Energy Storage Devices. *Prog. Polym. Sci.* **2023**, *143*.
171. Anupama Devi, V.K.; Shyam, R.; Palaniappan, A.; Jaiswal, A.K.; Oh, T.H.; Nathanael, A.J. Self-Healing Hydrogels: Preparation, Mechanism and Advancement in Biomedical Applications. *Polymers (Basel)*. **2021**, *13*.
172. Huang, S.; Wan, F.; Bi, S.; Zhu, J.; Niu, Z.; Chen, J. A Self-Healing Integrated All-in-One Zinc-Ion Battery. *Angew. Chemie - Int. Ed.* **2019**, *58*, doi:10.1002/anie.201814653.
173. Wang, X.; Wang, B.; Cheng, J. Multi-Healable, Mechanically Durable Double Cross-Linked Polyacrylamide Electrolyte Incorporating Hydrophobic Interactions for Dendrite-Free Flexible Zinc-Ion Batteries. *Adv. Funct. Mater.* **2023**, *33*, doi:10.1002/adfm.202304470.
174. Liu, J.; Long, J.; Shen, Z.; Jin, X.; Han, T.; Si, T.; Zhang, H. A Self-Healing Flexible Quasi-Solid Zinc-Ion Battery Using All-In-One Electrodes. *Adv. Sci.* **2021**, *8*, doi:10.1002/advs.202004689.
175. Li, Q.; Cui, X.; Pan, Q. Self-Healable Hydrogel Electrolyte toward High-Performance and Reliable Quasi-Solid-State Zn-MnO<sub>2</sub> Batteries. *ACS Appl. Mater. Interfaces* **2019**, *11*, doi:10.1021/acsaami.9b13553.
176. Liu, D.; Tang, Z.; Luo, L.; Yang, W.; Liu, Y.; Shen, Z.; Fan, X.H. Self-Healing Solid Polymer Electrolyte with High Ion Conductivity and Super Stretchability for All-Solid Zinc-Ion Batteries. *ACS Appl. Mater. Interfaces* **2021**, *13*, doi:10.1021/acsaami.1c09200.
177. Hong, L.; Wu, X.; Liu, Y.S.; Yu, C.; Liu, Y.; Sun, K.; Shen, C.; Huang, W.; Zhou, Y.; Chen, J.S.; et al. Self-Adapting and Self-Healing Hydrogel Interface with Fast Zn<sup>2+</sup> Transport Kinetics for Highly Reversible Zn Anodes. *Adv. Funct. Mater.* **2023**, *33*, doi:10.1002/adfm.202300952.
178. Long, J.; Han, T.; Lin, X.; Zhu, Y.; Ding, Y.; Liu, J.; Zhang, H. An Integrated Flexible Self-Healing Zn-Ion Battery Using Dendrite-Suppressible Hydrogel Electrolyte and Free-Standing Electrodes for Wearable Electronics. *Nano Res.* **2023**, *16*, doi:10.1007/s12274-023-5882-9.
179. Liu, Y.; Gao, A.; Hao, J.; Li, X.; Ling, J.; Yi, F.; Li, Q.; Shu, D. Soaking-Free and Self-Healing Hydrogel for Wearable Zinc-Ion Batteries. *Chem. Eng. J.* **2023**, *452*, doi:10.1016/j.cej.2022.139605.
180. Shen, P.; Hu, Y.; Ji, S.; Luo, H.; Zhai, C.; Yang, K. A Self-Healing Nanocomposite Hydrogel Electrolyte for Rechargeable Aqueous Zn-MnO<sub>2</sub> Battery. *Colloids Surfaces A Physicochem. Eng. Asp.* **2022**, *647*, doi:10.1016/j.colsurfa.2022.129195.
181. He, X.; Cheng, R.; Sun, X.; Xu, H.; Li, Z.; Sun, F.; Zhan, Y.; Zou, J.; Laine, R.M. Organic Cathode Materials for Rechargeable Magnesium-Ion Batteries: Fundamentals, Recent Advances, and Approaches to Optimization. *J. Magnes. Alloy.* **2023**, *11*.
182. Asif, M.; Kilian, S.; Rashad, M. Uncovering Electrochemistries of Rechargeable Magnesium-Ion Batteries at Low and High Temperatures. *Energy Storage Mater.* **2021**, *42*.
183. Liu, Q.; Wang, H.; Jiang, C.; Tang, Y. Multi-Ion Strategies towards Emerging Rechargeable Batteries with High Performance. *Energy Storage Mater.* **2019**, *23*.
184. Wu, X.; Dou, Y.; Lian, R.; Wang, Y.; Wei, Y. Understanding Rechargeable Magnesium Ion Batteries via First-Principles Computations: A Comprehensive Review. *Energy Storage Mater.* **2022**, *48*.

185. Ahn, H.; Kim, D.; Lee, M.; Nam, K.W. Challenges and Possibilities for Aqueous Battery Systems. *Commun. Mater.* **2023**, *4*.
186. Deivanayagam, R.; Ingram, B.J.; Shahbazian-Yassar, R. Progress in Development of Electrolytes for Magnesium Batteries. *Energy Storage Mater.* **2019**, *21*.
187. Li, M.; Ding, Y.; Sun, Y.; Ren, Y.; Yang, J.; Yin, B.; Li, H.; Zhang, S.; Ma, T. Emerging Rechargeable Aqueous Magnesium Ion Battery. *Mater. Reports Energy* **2022**, *2*.
188. Yang, G.; Xu, X.; Qu, G.; Deng, J.; Zhu, Y.; Fang, C.; Fontaine, O.; Hiralal, P.; Zheng, J.; Zhou, H. An Aqueous Magnesium-Ion Battery Working at  $-50\text{ }^{\circ}\text{C}$  Enabled by Modulating Electrolyte Structure. *Chem. Eng. J.* **2023**, *455*, doi:10.1016/j.cej.2022.140806.
189. Cheng, M.; Liu, J.; Wang, X.; Li, Y.; Xia, W.; Liu, Q.; Hu, J.; Wei, T.; Ling, Y.; Liu, B.; et al. In-Situ Synthesis of Bi Nanospheres Anchored in 3D Interconnected Cellulose Nanocrystal Derived Carbon Aerogel as Anode for High-Performance Mg-Ion Batteries. *Chem. Eng. J.* **2023**, *451*, doi:10.1016/j.cej.2022.138824.
190. Aziam, H.; Larhrib, B.; Hakim, C.; Sabi, N.; Ben Youcef, H.; Saadoune, I. Solid-State Electrolytes for beyond Lithium-Ion Batteries: A Review. *Renew. Sustain. Energy Rev.* **2022**, *167*, doi:10.1016/j.rser.2022.112694.
191. Wang, P.; Chen, Z.; Wang, H.; Ji, Z.; Feng, Y.; Wang, J.; Liu, J.; Hu, M.; Fei, J.; Gan, W.; et al. A High-Performance Flexible Aqueous Al Ion Rechargeable Battery with Long Cycle Life. *Energy Storage Mater.* **2020**, *25*, doi:10.1016/j.ensm.2019.09.038.
192. Wang, H.; Wang, P.; Ji, Z.; Chen, Z.; Wang, J.; Ling, W.; Liu, J.; Hu, M.; Zhi, C.; Huang, Y. Rechargeable Quasi-Solid-State Aqueous Hybrid  $\text{Al}^{3+}/\text{H}^{+}$  Battery with 10,000 Ultralong Cycle Stability and Smart Switching Capability. *Nano Res.* **2021**, *14*, doi:10.1007/s12274-021-3356-5.
193. Xiong, T.; He, B.; Zhou, T.; Wang, Z.; Wang, Z.; Xin, J.; Zhang, H.; Zhou, X.; Liu, Y.; Wei, L. Stretchable Fiber-Shaped Aqueous Aluminum Ion Batteries. *EcoMat* **2022**, *4*, doi:10.1002/eom2.12218.

**Disclaimer/Publisher's Note:** The statements, opinions and data contained in all publications are solely those of the individual author(s) and contributor(s) and not of MDPI and/or the editor(s). MDPI and/or the editor(s) disclaim responsibility for any injury to people or property resulting from any ideas, methods, instructions or products referred to in the content.